POLITECNICO
MILANO 1863

SCUOLA DI INGEGNERIA INDUSTRIALE E DELL'INFORMAZIONE
Corso di Laurea Magistrale in Ingegneria Meccanica

Finite Element Analysis of a ski for alpine touring

Relatore
Prof. Carlo Gorla

Correlatore
Ing. Luca Bonaiti

Candidato
Carlotta Maconi
Matr.919777

Anno Accademico 2019–2020

Politecnico di Milano:
www.polimi.it

Scuola di Ingegneria Industriale e dell'Informazione:
www.ingindinf.polimi.it

Acknowledgements

An authentic thanks to my relator Prof. Carlo Gorla, his teachings have been a true inspiration for my work. His passion for this wonderful sport increased my curiosity and desire to learn this discipline and complete a good work.

A deep thanks to Eng. Luca Bonaiti for the constant support and advices given during the whole thesis. His professional, but friendly behaviour was fundamental to create a real functional collaboration.

Notable thanks to SkiTrab company for the possibility to study physically its ski, sharing its technical details too.

Furthermore, I thank all the people who spent part of their time giving me useful tips and helping with the experimental tests.

Lecco, April 2021 Maconi, C.

«Da la meta mai non torcer gli occhi»
Alessandro Manzoni

Contents

List of Figures

List of Tables

Symbols

A	Area
β	Generalized coordinates
D	Nodal displacement vector
d_f	Fiber diamter
E	Young's Modulus
ε	Strain
η	Correction factor
G	Shear modulus
g	Internal D.o.F.
γ	Shear strain
J	Section of inertia
K	Stiffness matrix
L	Characteristic length
L_f	Fiber length
m	Mass
N	Shape function
ν	Poisson's coefficient
R	Loads vector
ρ_f	fiber density
ρ_m	matrix density
σ	Stress
T	Temperature
T_{g-PB}	Transition temperature of polybutadiene
T_{g-SAN}	Transition temperature of Acrylonitrile styrene
ϑ	Angular rotation
u	Displacement in x-direction
V	Volume
v	Displacement in y-direction
V_f	Fiber volume
w	Displacement in z-direction
w_f	Fiber weight fraction
w_m	Matrix weight fraction
ξ	Correction factor

Sommario

Questa tesi ha lo scopo di creare un modello affidabile per facilitare la prototipazione di sci permettendo alle aziende di progettare i loro prodotti in modo numerico tramite l'uso di software di simulazione ad elementi finiti, limitando la necessità di sperimentazioni, risparmiando tempo e denaro.

L'analisi è incentrata sugli sci d'alpinismo, ma può essere estesa a qualsiasi sci di diversa disciplina, semplicemente modificandone le proprietà e la forma, ma mantenendo valida la teoria alla base della connessione tra i materiali e i loro vincoli.

Dapprima è proposta una profonda analisi dei materiali. L'analisi riguarda lo stato dell'arte, sperimentazioni e dove è possibile viene affiancata una parte di simulazione. Questo modo di procedere permette di essere certi dei risultati sperimentali verificandone sempre la loro veridicità.

In secondo luogo si propone un confronto sulla deflessione ottenuta dalle prove di flessione e flesso-torsione, misurata tramite sperimentazione fisica e simulata usando un software ad elementi finiti, con lo scopo di raggiungere un buon livello di coerenza.

Parole chiave: Sci, Composito, Flessione, Flesso-torsione, Simulazione

Abstract

This thesis aims to create a reliable model to facilitate future ski prototipying allowing companies to design their products in a numerical way using Finite Element software, avoiding the need of experimental test, saving money and time.

This analysis is focused on ski touring, but it can be applied to every ski of different field simply by changing material properties and ski shape, but mantaining the theory about materials connections and constraints.

Firstly a deep analysis of the materials is proposed. The analysis regards state of the art, real experiment and where it is possible a simulation part. This step procedure allows to be sure of the simulation results, in fact it is mandatory to always verify their goodness.

Secondly a comparison of deflections caused by bending and bending-torsion measured through real tests and simulated using Finite Element software, aiming to achieve a proper level of coherence.

Keywords: Ski, Composite, Bending, Bending-torsion, Simulation

Introduction

History of ski comes from prehistoric age, mainly to facilitate mobility during hunt. During time its use was improved, arriving to the first military manuals about skiing technique in 1765, mainly focused on jumping and cross-country skiing. Only at the mid of nineteenth century ski was used with recreational function or in official racing. Important technological and coaching improvements took place along the whole century. Probably the most relevant was the introduction of carving skies and binding plates in 90s, by means of which higher inclination angles and tighter curves become possible, modifying significantly the approach to the sport.

Before entering in details about the technological requirements that a touring ski must provide (in terms of materials, construction and geometry), it is useful to briefly explain this sport. By means of this short explanation, it will be easier to understand why some solutions have been developed.

Ski touring combines elements of Nordic and alpine skiing, embracing a discipline called Telemark. It has been adopted seeking new snow and the joy of wonderful view. Respect to the more known alpine skiing, the characteristic feature and main difference, is the fact that both uphill and downhill are performed. That is because it tends to achieve higher height than the ones achievable with lifts. In order to leave a good freedom during hiking, boots are not strictly constrained with skies, the constraint is then used approaching downhill phase to ensure both safety and handling. It is obvious that a more complex architecture must be selected if compared to an alpine ski because both the phases, characterized by opposite requirements, must be accomplished.

By comparing the two types what it suddenly comes out is the difference in weight. Because touring ski must be led till the peak, the objective is a reduction of skier effort and so a lower weight is obviously preferred. On the other hand it is important to keep an high stiffness, fundamental during downhill.

The most complex part and core of the whole work is the correct modelling of ski, that has a multilayer structure. To proceed with the analysis, *"Ski Trab Freedom 90"* was used. It is a nine layers ski, simpler in terms of architecture than the one used for the Ski World Cup that arrives to fourteen layers.

The detailed analysis of the materials leads to a deep knowledge of ski performance and allows to evaluate possible improvements.

Chapter 1

Ski construction

Up to 1946, skies were basically constituted by wood. This solution showed many issues concerning weight, especially due to water absorption and change in shape, causing a worse mechanical resistance. With the adoption of a structure, already used in aeronautical field, ski was covered by two aluminium layers, resulting in a sort of sandwich shape. This innovation guarantees a reduction of wear for what concern ski edges, giving an important contribute to direction the turn on hard snow. From the 60s fibers were introduced, in combination with resins bring the born of a ski with higher stiffness and lower weight at the same time. Among the years development and continue research in materials remain a fundamental topic in ski evolution.

1.1 Materials

Skies manufacturing can vary quite a lot, although basic components are common to skies of every fields (alpine, ski touring and freestyle). Obviously, manufacturers use slightly different materials and methods in order to claim advantages on competitors, but, at the end, skies are built in accordance to the same basis.

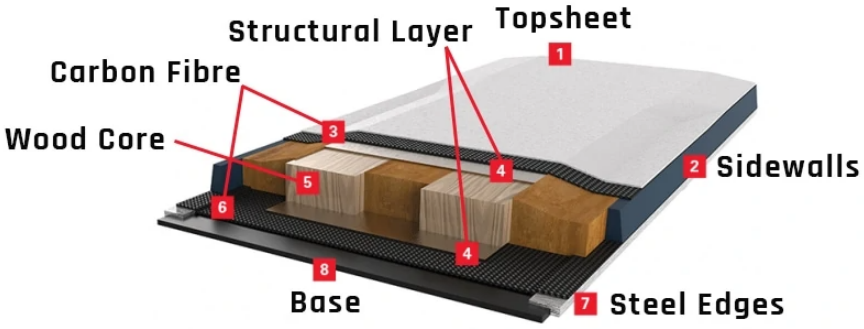

Figure 1.1: Common ski architecture. [1]

At the centre of any ski, as represented in Fig. 1.1, there is a laminated wood core or a combination core of wood and other materials. The core is usually surrounded by layers of composite materials, both above and below. A top sheet, base and

sidewalls are added, giving the ski its own distinctive characteristics. Finally, steel edges are added to help reinforcing and providing a better control.

1.1.1 Topsheet and base

Topsheet is the ski uppermost layer, where most brands logos or graphics are placed. Its main duty is to protect the inner composite layers and core. Topsheets are normally made from wood, fiberglass, nylon, plastic or a combination of materials.

On the other side of the ski, there is the base, which is typically made from polyethylene plastic. Polyethylene plastic are chains of ethylene monomer, that can be differentiated depending on density or looking to its molecular weight. For instance, there is the UHMWPE[1] (Ultra High Molecular Weight PolyEthylene). It is able to ensure a good combination of wear resistance and low friction coefficient, that are two fundamental requirements for the base, being subjected to abrasive surface like snow and ice. The combination with other elements allows an improvement of its mechanical properties. In particular, carbon increases its resistance from UV[2] radius, while silicon oil and talc reduce, again, friction coefficient. The cooling process must be executed slowly to ensure high quality of crystalline grain with volume reduction which allows the formation of microvoids useful for wax absorption. It can be obtained through three different processes: ram extrusion, compression molding and sintering. This last process characterizes the high quality bases because it allows high percentages of crystallization.

Sintered and *Extruded* are the terms usually used in regards to bases. Extruded base material is made by melting down polyethylene pellets to a viscous state, followed by compression into sheets. This method is more cost effective but the final product is slower, holds less wax and less durable. Sintered bases are made by compressing and heating polyethylene powder without reaching the melting point. As result the final product will be more porous and durable.

1.1.2 Core materials

Core materials represent the most relevant part of the ski, giving strength and stiffness. They also provide the damping effect, that is a fundamental aspect while skiing on a rough surface. Laminated wood cores have been, and still remain, the gold standard in ski construction. Wood is a natural composite formed by a complex chain of cellulose cells, reinforced by polymeric substance known as lignin, as well as other organic compounds. One of the variables in wood structure is represented by humidity percentage. It is defined as:

$$\%humidity = \frac{weight\ of\ water\ in\ the\ specimen}{weight\ of\ the\ specimen\ of\ the\ dried\ wood} \tag{1.1}$$

Humidity can achieve a value up to 200% and it affects the elasticity and impact resistance. Usually with the term dried wood, a humidity of about 12% is indicated. The compression resistance in the same direction of the fiber is more

[1] Ultra High Molecular Weight PolyEthylene
[2] Ultraviolet Radiation

or less ten times higher than the resistance in transversal direction and the reason is related to the strong covalent bonds between cellulose cells, mainly oriented in the longitudinal directions. While in perpendicular direction, lateral hydrogen bonds between cellulose cells leads to a lower mechanical resistance. Thanks to its elasticity and the independence from temperature variation, wood guarantees a great stability, as well as good damping properties if compared to other plastic materials.

Woods can be divided in two main categories, hard wood and soft wood, depending on their strength (Fig. 1.2).

Figure 1.2: Wood used in the ski construction.

A laminated wood core is made of cut strips of wood, glued and pressed together. Beech, Maple, Ash, Poplar and Aspen are among the most popular woods used in cores today for the majority of ski categories. Commonly they are blended together to achieve a more balanced feel. Harder, more dense woods will give ski a stiffer and more durable feel. They are often used in hard charging skies where weight is less of a factor. Dense hard woods means longer fibers, allowing more energy to be stored entering a turn and more released energy exiting a turn. Less dense woods gives the ski a more playful and forgiving feel, better for whipping around in tight spaces and handling off-tracks.

Typically, lighter kind of wood, like Paulownia, Bamboo and Balsa are selected for touring skies because they reduce the overall weight. A light ski is perfect for uphill phase, but its performance during downhill will be sacrificed, as the ski will be less damped and with less edge grip in firmer conditions.

One possible alternative to wood is represented by polymeric foams, with the great advantage of weight reduction but with lower efficiency. For this reason only low-medium level of skies are realized with it. In ski field the most used are expanded polymeric foams with density between 20 - 400 $\frac{Kg}{m^3}$. In detail PU[3] (polyurethanic foam) is the reference category, showing a good adhesion property to all materials and a range of temperature application between -200° and 150°C. PU cores can be combined with wood for a "hybrid" approach, in order to combine lightweight and playful nature while having energy and dampness. The foam cores are typically encapsulated in a Cap construction that rolls over the top down to the metal edge. The major disadvantage is on manufacturing side. The production phase consists in filling precisely a fixed cavity without the possibility of adding or subtracting material. This can make the prototyping phase very expensive and cost savings of manufacturing injected skies become relevant only with high quantities.

[3]Polyurethanic foams

1.1.3 Structural layers

With the term structural layers, the reference is to those layers used above and below the wood cores, affecting the dampness, energy and torsional stiffness, basically the flavour profile of the ski. Among all materials the most important are presented.

Fiberglass is the most widely used composite in ski industry. It's cost-effective, easy to manufacture and provides energy and responsiveness when combined with a wood core. Once combined with epoxy resin (which is then heated and pressed), it becomes extremely strong, improving longitudinal and torsional stiffness, essentially strengthening the ski to reduce chatter [4]. On the other side it is heavy (after being saturated in epoxy) and degrades over time.

Carbon Fiber is used in the same way as fiberglass, but is much lighter and generates more energy. Unfortunately, these benefits leads to a much higher manufacturing cost, explaining why carbon fiber strands occurs only on top of the wood core (instead of full layers that run over the entire core). Carbon is worse in terms of vibrations absorption than fiberglass, so it is important to set the right ratio ensuring balance with a wood core with good damping properties, otherwise the vibration will be increased leading to a ski nervous or chattery.

Fiber reinforced materials will be analysed deeply in Chapter 2 because their mechanical properties and combination are different from the simple isotropic materials usually discussed and needs to be clarified.

Titanal is an aluminium alloy that represents the most common metal in skies. Plain and simple, Titanal adds power, stability and dampness. It is typically found in more aggressive all-mountain skies because of the added strength and grip on harder snow. Titanal can be used in full sheets above and below the core or in form of strips in certain sections. This last tendency is becoming more and more popular thanks to the overall reduction of ski weight.

1.1.4 Sidewalls

If present, sidewalls run along the ski length, directly above the metal edge. ABS[5](Acrylonitrile Butadiene Styrene) sidewalls are present in Sandwich and Half-Cap architectures.

ABS is a common thermoplastic polymer made by polymerizing styrene (40-60%) and acrylonitrile (15-35%) in the presence of polybutadiene(5-30%). thanks to the optimum mechanical properties, it represents one of the finest mix between elastomer and resin.

The advantage of ABS is to combine the stiffness and strength of Acrylonitrile styrene, that is amorphous at environmental temperature, with the elasticity of polybutadiene, which is instead rubbery. In this way the material obtained is a biphasic, whose behaviour depends on temperature. In particular at T<T_{g-PB} both the components are amorphous and material will be characterized by high stiffness and so brittleness, while at T>T_{g-PB}, that represents a common thermic

[4]Chatter is the continuous engaging and disengaging of ski tip edges, which results in a "chattering" sound. Ski tip flaps up and down rapidly.

[5]Acrylonitrile Butadiene Styrene

field, matrix is amorphous while phase is rubbery. Thanks to the amount of polybutadiene, material keeps its mechanical resistance and a Young's modulus in the order of some GPa. Finally at T>T_{g-SAN} matrix and phase are rubbery and the Young's Modulus results in MPa field.

The presence of a biphasic structure makes the material stiff and tough even at low temperature, with great impact resistance. All these features makes ABS essential to protect the ski inner part, guaranteeing, at the same time, a certain flexibility to follow ski deformation.

1.1.5 Steel edges

Manufacturers install a metal edge between the base and lower composite layers to reinforce the ski and facilitate skiing action in case of hard snow. For what concerning edge construction, skies can be characterized by full or partial wrap. The first solution is used to gain strength, while the second is preferred thanks to its lightness and its easier maintenance in case of damage. There are two options referring to edge thickness:

1. thicker edge is more durable and will hold up better when hitting rocks or trees;

2. thinner edge which may glide faster, but is more vulnerable to bending or breaking in case of obstacles.

1.1.6 Resin

Resin can be distinguished between thermoset and thermoplastic. The one used in ski construction are thermoset. Epoxy resins are one of the available thermosetting polymers, that means solidification through chemical reactions, in which polymer chains are bonded to each other by means of covalent cross-links, making the resin insoluble and infusible once hardened. Epoxy groups ring conformation gives stiffness and heat resistance by better absorbing mechanical stresses compared to a linear polymer chain. At chain ends, reactive groups are connected to hardening agents, the amines, which are part of the cross-linking process, forming a very dense three-dimensional mesh.

Identifiable by their amber or brown colour (unlike other thermosetting resins that use a catalyst to trigger crosslinking process), epoxy resins must be mixed with hardening agent in the right proportion to ensure the desired thermal resistance and chemical characteristics. The greater adhesion property of epoxy resins, if compared to other resins, for making composites allows to obtain very high cohesion but with much lower quantities of resin, improving final product lightness. Thanks to this quality, the use of epoxy resins is particularly suitable for making honeycomb sandwich cores.

The development of technology, adhesion and tenacity characteristics of epoxy polymer allows to obtain an efficient and resistive adhesive, suitable to make real structural connections replacing mechanical ones.

1.2 Construction technique

Another fundamental feature is how materials are arranged together. Three main schemes construction are used:

- ABS Sidewall/Sandwich Construction (Fig. 1.3)
- Cap Construction (Fig. 1.4)
- Half-Cap Construction (Fig. 1.5)

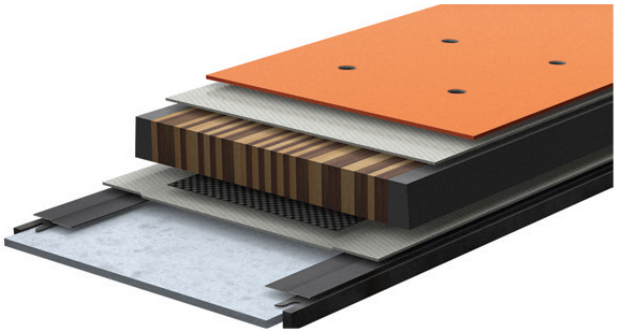

Figure 1.3: Sandwich construction. [2]

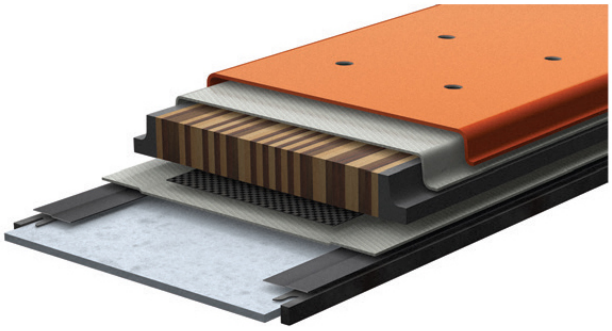

Figure 1.4: Cap construction. [2]

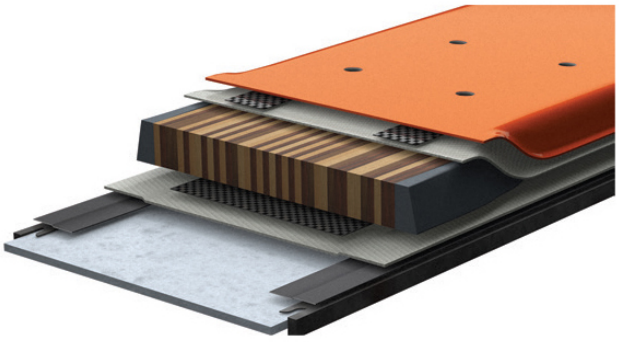

Figure 1.5: Half-Cap construction. [2]

1.2.1 Sandwich construction

This configuration, shown in Fig. 1.3, is the most performing but, at the same time, the most expensive one. It ensures high level of axial and torsional stiffness providing good stability and handling at high speed. The main role is played by sidewalls that consist of dense plastic (ABS) used to prevent damages, guaranteeing integrity of the core and fundamental for transmitting skier force on the edge lamina. This characteristic is mechanically explained with a higher torsional rigidity, edges will be rigid, rather than deflecting off the snow, and globally, ski will be less prone to edge compression. The downside is that the higher density brings higher weight, that is a delicate issue in ski touring, but an affordable factor in ski alpine.

1.2.2 Cap construction

It represents an opposite configuration respect to Sandwich construction. It was firstly introduced in 1989 and as can be seen in Fig. 1.4, does not utilize sidewalls. In order to hold ski sides together, this technology has the topsheet material fold over the top of core material and around its sides, creating a rounded appearance. Cap construction skies are not the most reliable in terms of edge holding. These skies can feel very flimsy and bounce off the snow, rather than grip the snow and stay stable. Its most important benefit is its lightness, making it particularly suitable for dedicated touring and long ascents. This choice is approached mainly to have skies easy to use with lower axial stiffness, but acceptable torsional one thanks to the presence of a kind of torsion box.

A particular attention is required, being the construction method of the ski that will be analysed in next chapters.

1.2.3 Half-Cap construction

Fig. 1.5 shows an hybrid construction option, using areas of sidewall, and areas of cap construction. It is characterized by much shorter pieces of sidewall that are placed directly in the ski centre (where ski is more subjected to forces, receiving an higher amount of energy input from the athlete). After the short sidewall section underfoot, a torsional box is used at the tip and tail of the ski. Overall, this architecture gives to the ski an area of torsional rigidity and strength underfoot, saving some weight by not utilizing sidewalls for about half of the running length. Due to the lack of sidewalls along all the length, it is still difficult to fully use the edges of the ski to drive a turn. Specifically, in case of a sharp turn, semi-cap skies tends to wash out of the turn rather than engage the edge upper portion to cleanly tighten the turn.

1.3 Geometry

Together with materials assembly, another important aspect is the global geometry. This term refers to ski camber and radius.

1.3.1 Camber

Camber plays a huge role in the performance of any ski, it describes the curvature of a ski in a lateral view. Camber is evident when unweighted, then once applied the load, it becomes neutralized and flat against the snow. Its importance is related to the reduction of pressure under the bindings, making maneuvering of skies easier and adding a sort of spring action to turns and pop for jumps.

All the possible configurations are here listed:

- Full camber/traditional camber
- Tip Rocker
- Tip and Tail Rocker
- Full Rocker

Before entering in the detailed description of the different types, it is better to introduce the term of effective edge, fundamental in understanding which configuration is the best in terms of control. Effective edge is the edge engagement length on hard snow.

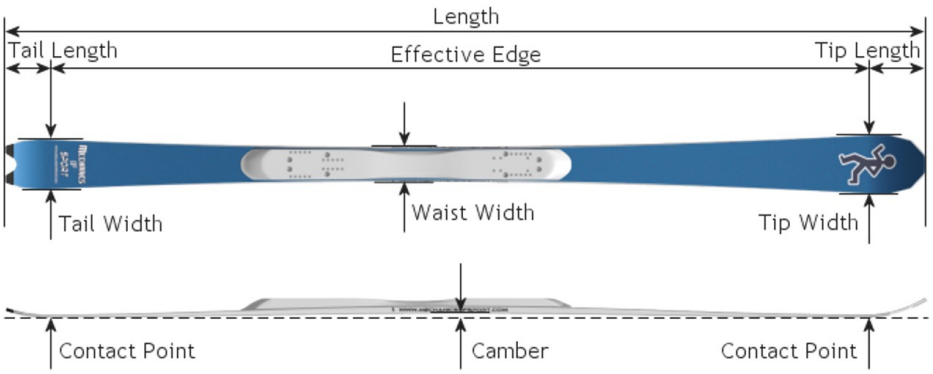

Figure 1.6: Edge effective. [3]

An easy way to determine a ski effective edge length, as underlined in Fig. 1.6, is to place the ski base-to-base, or on a flat surface, and depress the camber. The contact points of tip and tail are the positions where the edges begin to turn up. That length, in between the tip and tail, is the effective edge.

Any ski with a very short effective edge is unstable and slippery at higher speeds. In choppy, variable conditions or ice, a ski with this kind of characteristics, does not hold the edge as well as a ski with a longer one. On other hand this type of ski will excel in soft snow and powder, resulting easy to pivot in tight trees and technical lines.

A longer effective edge is very stable at higher speeds, but in case of softer snow, the ski appears difficult to move. Propensity to ski below the snow surface, especially in powder, will be increased affecting the quality of quick maneuvers.

From Fig. 1.7 to 1.10 the different geometries are proposed in order to offer a better understanding of the below description.

Traditional camber

The ski arches into air, thanks to the two extremes that are in contact with the snow. This configuration allows to push all the ski length on snow once weighted, providing the most edge contact and grip possible on hard packed snow [6] translating in a better control and stability. This is the typical design chosen for ski racing where control is the key, because the ski will cut the snow without floating on it.

Tip Rocker

A tip rocker or early rise tip is characterized by a first rise of the ski profile before the real tip starts. Tip Rocker helps the ski to float in powder, exploiting the upward section to climb over soft snow. However, it worsens the performance on track due to a lower ski edge contact with the snow, when the ski is flat or leant over at smaller angles. A less pronounced rocker shape can be chosen to make changing from one edge to the other easier on hard packed snow, without affecting too much the edge grip.

Tip and Tail Rocker

Skies with a tip and tail rocker have a reduced area of positive camber in the middle section, but with rocker sections towards both the tip and tail. The length of these sections can change, making the area of positive camber longer or shorter, in order to move the centre of positive camber more towards the middle or back of the ski. Depending on the camber shape the ski can be more oriented to powder skiing, or on the other hand, retaining better control on the track.

Full Rocker

A full rocker, also known as reverse camber ski, has a flat camber in the middle and both ends arc upward, away from the snow. This shape makes the ski very good at floating in powder, whether skiing forwards or backwards, but due to the flat camber section, does not provide so much grip on hard packed snow.

[6] Hard-packed snow is a type of snow that for skiers, and particularly for snowboarders, appears challenging especially for turning ensuring a good grip

Figure 1.7: Traditional Camber. [3]

Figure 1.8: Tip Rocker. [3]

Figure 1.9: Tip and Tail Rocker. [3]

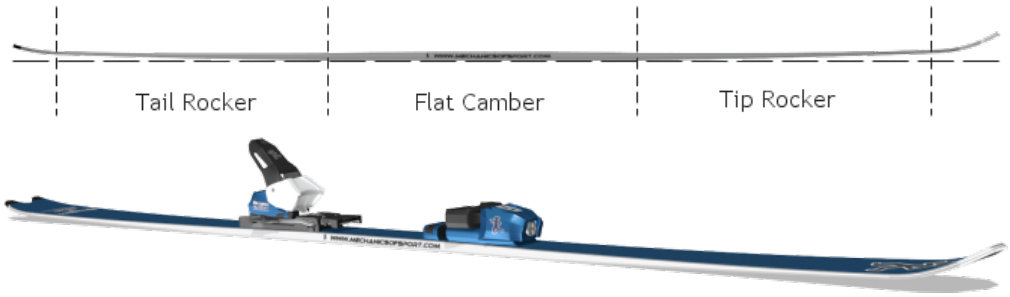

Figure 1.10: Full Rocker. [3]

1.3.2 Turn Radius

The term "turn radius" refers to the sidecut, that can be defined as the radius of a circle tangent to ski edge, or as alternative is defined as the curvature of the ski edge from tip to tail. Both the interpretations are depicted in Fig. 1.11.

It is essential in ski choice because it characterizes its natural tendency to turn. The lower the turn radius value, the more “turny” a ski is going to be, while higher value means a “straight line behaviour" characterized by longer turns and faster skiing.

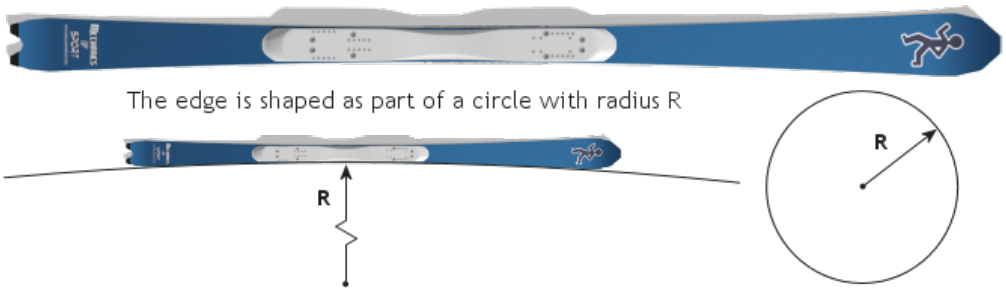

Figure 1.11: Sidecut. [3]

Referring to some numbers, Short turn radius is 10-15 m, medium is 15-20 m and long is more than 20 m. These are general indications, because also length plays an important role in this distinction.

1.4 Conclusions

In this chapter, the historical development of the ski from the technical point of view is underlined, starting from materials up to construction and geometry. It has been explained briefly the reasons behind different ski assemblies, allowing to understand its full potentialities by simply looking to its genetic code. Materials and geometry must be considered as interconnected worlds, whose choice are relevant and influence each other.

Chapter 2

Fiber reinforced composite for ski

[1] Among all the materials used in ski production a special attention is given to composites. The motives are related to the increasing use of this kind of material especially in sport field. They were firstly introduced to replace all those heavy elements, thanks to some relevant aspects in terms of weight, mechanical performance and design. Weight is a critical factor that affects deeply the performance, so lightness represents a relevant advantage.

At the same time, fiber reinforced composite material guarantees high elastic modulus, suitable in sports equipment thanks to the enhanced elastic behaviour, ensuring a good damping shock absorption. Finally, also in terms of design, there is more freedom with associated low cost maintenance if compared to other materials.

2.1 Composites

The major constituents in a fiber-reinforced composite material are reinforcing fibers and matrix. Fibers are the principal load-carrying members, while the surrounding matrix keeps them in the desired location and orientation, acting as a load transfer medium and ensuring protection from environmental damages and humidity. The principal fibers in commercial use are glass, carbon and aramid. Depending on the application, the matrix can be polymer, metal or ceramic.

The reason why composites are a solution more and more adopted in many engineering fields is related to the combination of strength and modulus that are comparable or better than many traditional metallic materials. The greatest advantages are in terms of low density, strength-weight ratios and modulus-weight ratios, in addition fatigue strength as well as fatigue damage tolerance of many composites are excellent. Differently from classical materials such as metals, composites show a non-isotropic behaviour.

As consequence of this non-isotropy, their properties depend strongly on the direction of measurement, in fact tensile strength and modulus of an unidirectionally oriented composite are maximum when these are measured in the longitudinal direction of fibers. Similar considerations refer to other mechanical and thermal properties, such as impact strength coefficient of thermal expansion and thermal

[1] The main literature references for this chapter are: *Fiber-reinforced composites: materials, manufacturing, and design* [4] and *Handbook of Technical Textiles* [5].

conductivity. Although unidirectional composite properties in other directions are lower, they still represent a considerable advantage over common structural metals on a unit weight basis. Futhermore, the difference of properties in different directions creates a unique opportunity of tailoring them according to the design requirements.

The use of fiber-reinforced polymer as skin material combined with a lightweight core allows a further degree of design flexibility that is not easily achievable with metals. The sandwich construction, that is applied also in this case study, can produce high stiffness with very little, if any, increase in weight. The heterogeneous nature of these materials provides mechanisms for energy absorption on a microscopic scale, which is comparable to the yielding process. Depending on the type and severity of external loads, a composite laminate may exhibit gradual deterioration in properties but, usually, a composite would not fail in a catastrophic manner. Another unique characteristic of many fiber-reinforced composites is their high internal damping. This leads to better vibrational energy absorption within the material, resulting in reduced transmission of noise and vibrations to neighbouring structures.

This brief description aims to underline why for ski design, the use of fiber-reinforced composites is mandatory, from the point of view of mechanical properties and weight till the high damping absorption. Before characterizing every possible fiber configuration, it is important to present some general properties. As previously introduced, composites are orthotropic materials, which means that their properties are not the same for all directions, but three orthogonal planes of properties symmetry exist. The intersection of these three planes determine three principal directions (1,2,3) as showed in Fig. 2.1.

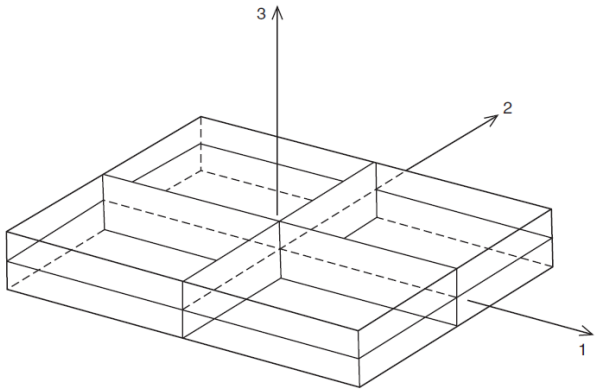

Figure 2.1: Principal directions construction.

For an isotropic material, the constitutive law can be described as:

$$\varepsilon_1 = \frac{1}{E} \cdot (\sigma_1 - \upsilon \cdot (\sigma_2 + \sigma_3)) \tag{2.1a}$$

$$\varepsilon_2 = \frac{1}{E} \cdot (\sigma_2 - \upsilon \cdot (\sigma_1 + \sigma_3)) \tag{2.1b}$$

$$\varepsilon_3 = \frac{1}{E} \cdot (\sigma_3 - \upsilon \cdot (\sigma_1 + \sigma_2)) \tag{2.1c}$$

While for a composite, the basic law will be determined by a different constitutive matrix, that is characterized by the presence of new constants that are E_1, E_2, E_3, ν_{12}, ν_{23}, ν_{13}, G_{12}, G_{23} and G_{13}. To relate the strain and stress, constitutive matrix is used.

$$\begin{bmatrix} \varepsilon_1 \\ \varepsilon_2 \\ \varepsilon_3 \\ \varepsilon_4 \\ \varepsilon_5 \\ \varepsilon_6 \end{bmatrix} = \begin{bmatrix} \frac{1}{E_1} & -\frac{v_{21}}{E_2} & -\frac{v_{31}}{E_3} & 0 & 0 & 0 \\ -\frac{v_{12}}{E_1} & \frac{1}{E_2} & -\frac{v_{32}}{E_3} & 0 & 0 & 0 \\ -\frac{v_{13}}{E_1} & -\frac{v_{23}}{E_2} & -\frac{1}{E_3} & 0 & 0 & 0 \\ 0 & 0 & 0 & \frac{1}{G_{23}} & 0 & 0 \\ 0 & 0 & 0 & 0 & \frac{1}{G_{13}} & 0 \\ 0 & 0 & 0 & 0 & 0 & \frac{1}{G_{12}} \end{bmatrix} \begin{bmatrix} \sigma_1 \\ \sigma_2 \\ \sigma_3 \\ \sigma_4 \\ \sigma_5 \\ \sigma_6 \end{bmatrix} \tag{2.2}$$

An important but reasonable simplification can be done and is related to the consideration of plane stress. In fact studying a component that has a small thickness compared to its length, it is possible to consider that in-plane stresses are different from zero, while the others are null. Obviously, deformation in the third direction is not zero due to the tridimensional deformation field related to the Poisson's effect. So, it is a state of stress in which normal stresses and shear stresses directed perpendicular to the plane of the body are assumed to be zero. By increasing plate thickness, the real state of stress switches from plane stress to plane strain. By this assumption, the matrix previously written becomes:

$$\begin{bmatrix} \varepsilon_1 \\ \varepsilon_2 \\ \varepsilon_6 \end{bmatrix} = \begin{bmatrix} \frac{1}{E_1} & 0 & 0 \\ -\frac{v_{12}}{E_1} & \frac{1}{E_2} & -\frac{v_{32}}{E_3} \\ 0 & 0 & \frac{1}{G_{12}} \end{bmatrix} \begin{bmatrix} \sigma_1 \\ \sigma_2 \\ \sigma_6 \end{bmatrix} \tag{2.3}$$

The resuming constants that need to be calculated are E_1, E_2, ν_{12}, G_{12}. These constants can be found experimentally or by using the Rule of mixture. Their experimental determination will be treated in the following Ch. 5, while the theoretical rule is here presented.

$$E_1 = E_f \cdot V_f + E_m \cdot V_m \tag{2.4a}$$

$$\frac{1}{E_2} = \frac{1}{E_f} \cdot V_f + \frac{1}{E_m} \cdot V_m \tag{2.4b}$$

$$\nu_{12} = \nu_f \cdot V_f + \nu_m \cdot V_m \tag{2.4c}$$

$$\frac{1}{G_{12}} = \frac{1}{G_f} \cdot V_f + \frac{1}{G_m} \cdot V_m \tag{2.4d}$$

V_f represents the fiber volume fraction that is

$$V_f = \frac{V_f}{V} = \frac{w_f \rho_f}{w_f \rho_f + w_m \rho_m} \tag{2.5}$$

In which w_f represents the fiber weight fraction, w_m matrix weight fraction and ρ_f is the fiber density while ρ_m is matrix density. The rule of mixture appears to be really useful but it is based on some important assumptions:

1. fibers and matrix are orthotropic materials;
2. fibers are uniformly distributed in the matrix;
3. fibers are perfectly aligned in one direction;
4. composite laminae are free of voids.

It is easy to understand that the above conditions are ideal. To correct approximate the reality Halpin-Tsai correction must be applied. As a result E_2, G_{12} are calculated in this way:

$$\frac{E_2}{E_m} = \frac{1 + \xi\eta V_f}{1 - \eta V_f} \tag{2.6}$$

In which $\eta = \dfrac{\frac{E_f}{E_m} - 1}{\frac{E_f}{E_m} + \xi}$ with $\xi = 2$

$$\frac{G_{12}}{G_m} = \frac{1 + \xi\eta V_f}{1 - \eta V_f} \tag{2.7}$$

In which $\eta = \dfrac{\frac{G_f}{G_m} - 1}{\frac{G_f}{G_m} + \xi}$ with $\xi = 1$

While in case in unidirectional discontinuous fiber the rule changes the formula for E_1 also, it becomes:

$$\frac{E_1}{E_m} = \frac{1 + \xi\eta V_f}{1 - \eta V_f} \tag{2.8}$$

With $\eta = \frac{\frac{E_f}{E_m} - 1}{\frac{E_f}{E_m} + \xi}$ with $\xi = \dfrac{2L_f}{d_f}$

2.1.1 Textile reinforced composites

The general description given in the below section aims to present the structure and complexity of this material class, in which fiber orientation plays a significant role in defining its behaviour. There are a lot of possible fiber combinations, each of them is specific of its structural use:

- Unidirectional reinforced composites
- Woven fabric-reinforced composites
- Braided reinforcement
- Knitted reinforcement
- Stictched fabrics
- Mat

Unidirectional reinforced composites

This class of composite represents the base in composite field. Its mechanical properties can be described, with good approximation, with Eq. 2.4. Under this assumption it is useful to compare the mechanical properties of the main fiber materials.

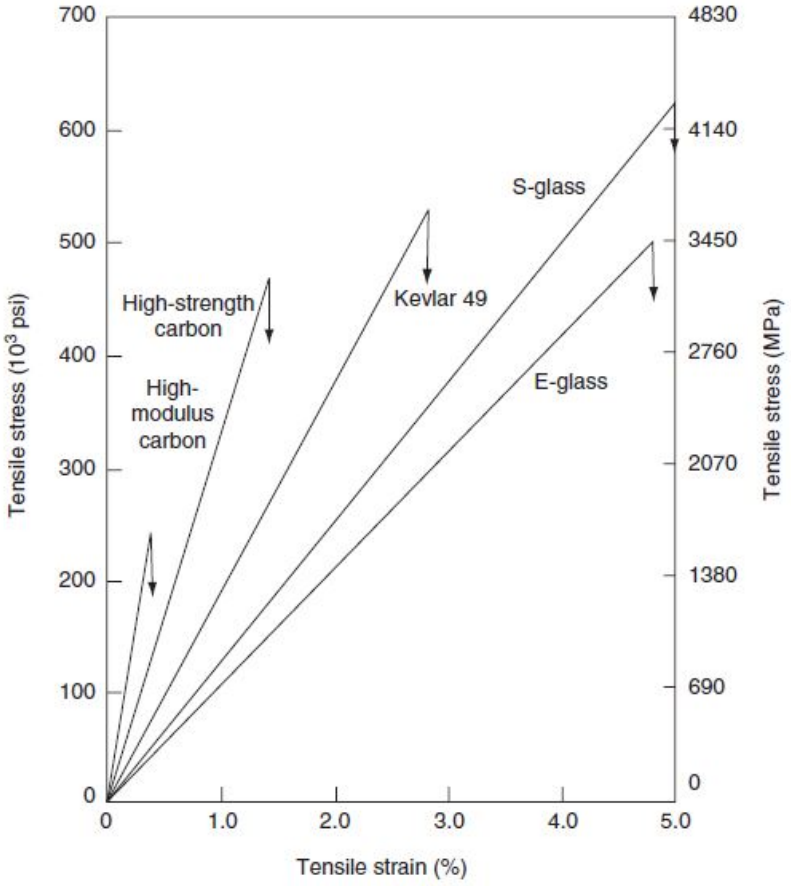

Figure 2.2: Tensile stress–strain diagrams obtained from single filament test of reinforcing fibers. [4]

Fig. 2.2 highlights big differences among the most common reinforcement materials. In particular, glass fibers are the most used for polymeric matrix composites. The principal advantage is offered by their low cost, allowing high tensile strength, high mechanical resistance and excellent insulating properties too. The disadvantages are relatively low tensile modulus and high density, sensitivity to abrasion during handling, high hardness (which causes excessive wear on molding dies) and low fatigue resistance. Glass fibers can be divided in two categories:

1. E-glass: it has the lowest cost and this is the reason beyond its spread use;
2. S-glass: it has the highest tensile strength, but with big manufacturing costs.

Carbon fibers are available in different modulus range from 207 GPa to 1035 GPa. They present advantages in terms of high tensile strength-weight ratio, high tensile modulus-weight ratios and very low coefficient of thermal expansion. In addition,

they are characterized by high fatigue strength and high thermal conductivity, but low impact resistance and strain to failure. Their high cost makes them more used in aerospace and automotive industry.

Finally, Aramid fibers are highly crystalline aromatic polyamide fibers with the lowest density and highest tensile strength-to-weight ratio. They are more known as Kevlar. Their field of interest is marine and aerospace applications where lightweight, high tensile strength and resistance to impact damage are important. On the other hand compressive strength is low and they are difficult to machine.

Woven fabric-reinforced composites

Woven fabrics, characterised by the interlacing of two or more yarn systems, are currently the most widely used textile reinforcement with glass, carbon and aramid as reinforcing fiber. Woven reinforcement exhibits good stability in the warp and weft directions and offers the highest cover or yarn packing density in relation to fabric thickness. They also show an increased resistance to impact damage compared to nonwoven composites, with significant improvements in compressive strengths after impact. Different architectures are available, mainly based warp and weft fibers paths and the way they are arranged together. Fig. 2.3 presents some examples.

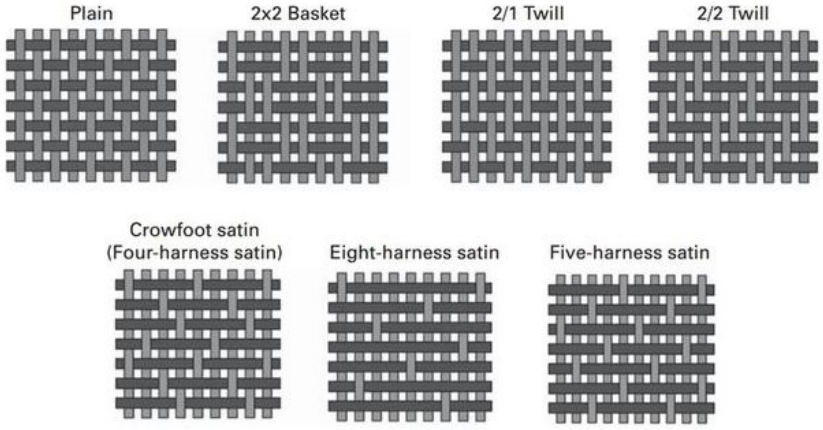

Figure 2.3: Possible woven architectures.

Braided reinforcement

Braided textiles for composites consist of intertwined two (or more) sets of yarns, one set of yarns being the axial yarns. In two-dimensional braiding, the braided yarns are introduced forming a certain angle with the axial direction and the intertwining is often in 1x1 or 2x2 patterns. The braided architecture enables the composite to endure twisting, shearing and impact better than woven fabrics. The stability or conformability of the braided structure depends on the detailed fibre architecture. Generally, the mechanical properties of composites fabricated using braided reinforcement depend on the braid parameters (braid architecture, yarn size and spacing, fibre volume fraction) and on the mechanical properties of fibre and matrix. Possible configurations are shown in Fig. 2.4.

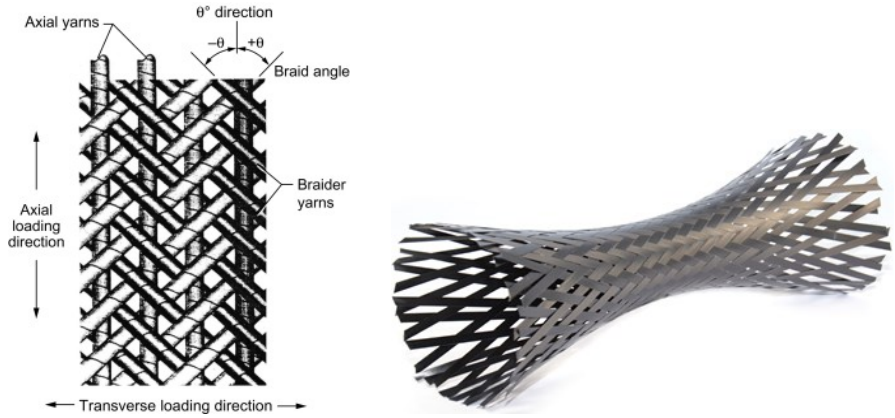

Figure 2.4: Braided Reinforcement [5]

Knitted reinforcement

The major advantages of knitted fabric-reinforced composites are the possibility of producing net shape preforms and the exceptional drapability of the fabrics, allowing more complex shapes. The interlooped nature of the reinforcing fibres/yarns permits the fabric to have the stretchability to adapt to complex shapes without crimp. On the other hand the in-plane stiffness and strength of the composites is reduced due to the relatively poor use of the mechanical properties of the fibre. Fig. 2.5 shows possible yarn loops configurations.

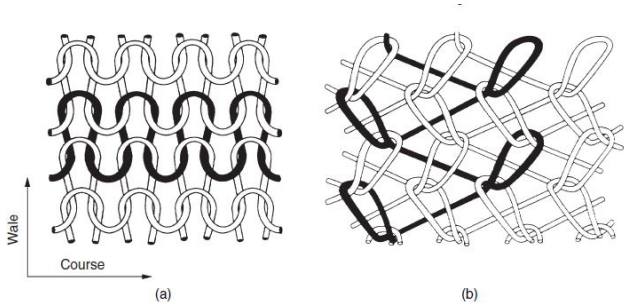

Figure 2.5: Knitted reinforcement. [5]

Stitched fabrics

Stitching composites has been seen as a direct approach to improve the through thickness strength of the materials. This increases their damage tolerance that is usually triggered by microbuckling in the vicinity of a delamination.

Considering the production process stitching of composites adds one further production step with the use of a sewing machine to introduce lock stitches through the full thickness of the laminate. The stitching can be performed on unimpregnated fibres or fibres in the prepreg form, usually done to avoid excessive fibre damage. In its more sophisticated form, stitches are used to produce a fabric which consists of warp (0°), weft (90°) and (optionally) bias ($\pm\vartheta$) yarns held together by the warp-knitted stitches, which usually consist of a light polyester yarn. The resulting

fabric is called a NCF[2] (non-crimp fabric) or MWK[3] (multiaxial warp-knit fabric). Fig. 2.6 proposes an example of stitched fabric.

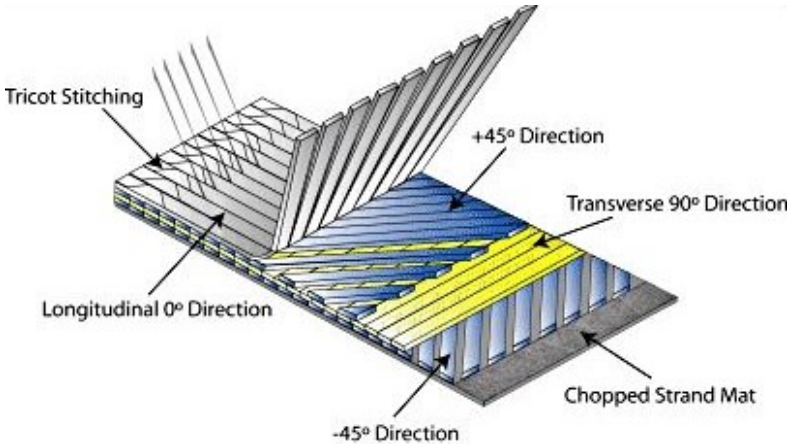

Figure 2.6: Stitched fabrics. [6]

Mat

Mat is a random fiber textile that provides equal strength in all directions and is used in a variety of hand lay-up and open-mold applications. It can be divided depending on the length of the fibers. CSM[4] (Chopped strand mat) is produced by chopping continuous strand roving into short lengths and dispersing the cut fibers randomly over a moving belt to form a "sheet" of random fiber mat. Thanks to random fiber orientation, chopped strand mat conforms easily to complex shapes, in addition it can absorb resin for two or three times its weight. For this reason, it is commonly used to repair chassis of boats, offering good strength and chemical resistance. This tendency can be enhanced by its thickness and weight. Continuous filament mat instead, is composed by long strands in multiple layers held together by a proper binder. Respect to other mats, with the same amount of resin and fibers, they show better mechanical properties of about 15-20%. CSM and continuous filament are displayed in Fig. 2.7.

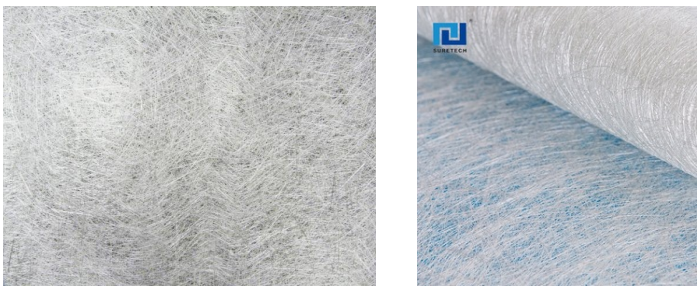

Figure 2.7: Random fiber orientation.

[2]Non-crimp fabric
[3]Multiaxial warp-knit fabric
[4]Chopped strand mat

The main advantage offered by the random orientation of fibers is guaranteeing an isotropic behaviour in the plane of the lamina. In fact, knowing the theory of composites, considering a lamina with such orientations the tensile modulus and shear modulus can be calculated as:

$$E_{random} = \frac{3}{8}E_1 + \frac{5}{8}E_2 \tag{2.9a}$$

$$G_{random} = \frac{1}{8}E_1 + \frac{1}{4}E_2 \tag{2.9b}$$

$$\upsilon_{random} = \frac{E_{random}}{2G} - 1 \tag{2.9c}$$

where E_1 and E_2 are the moduli calculated assuming a unidirectional fibers composite as reported in Equation 2.4.

2.2 Conclusions

The role of composite in the ski field is becoming more and more important. Their proper combination with metal element can improve greatly ski performance. However, not all the textile reinforcement are similar, depending on the purpose, some types of reinforcement and combinations are selected. This is the great advantage of composites, being able to achieve the desired mechanical behaviour by changing its geometry or fibers ensuring weight saving. In this chapter, the theory about composites was investigated, starting from a general study and going in detail to the most used configurations.

Chapter 3

Loads during performance

In order to qualify the performance of a ski, it is useful to test it by imposing the real forces acting during skiing. The easiest behaviour to be evaluated is the response to bending action. The feeling of ski flex is gained by supporting the shovel with one hand and pushing on the binding area. This is an example of a very simplified version of three point bending test and it flexes the ski longitudinally. More difficult, but fundamental too, is evaluating torsion. Manually, it can be tested by gripping the ski at binding toe and twisting the tip.

These are two simple operations that give an indication about model stiffness. Depending on the level of experience of the skier different flexural and torsional response will be selected. For this reason it is interesting to understand why and in which conditions these two parameters become fundamental.

3.1 Bending

Ski bending consists in deflection in the same plane of load application point. This phenomena can happen in two main situation during skiing: it may be caused by skier weight when there are two bumps and the ski is in the middle (with tip and tail on the bumps) or while the ski turns due to the effect of skier weight and edge angle.

This second situation is obviously more interesting and fundamental in the correct skiing mechanic. When turning, bending is not a preliminary attitude among skiers. In fact, turning could rely only on shape and sidecut without being in control of the speed and turning direction (railing). In this case, smaller radius are determinant for smaller turns. To have higher control on ski, bending must be introduced. Railing and correct turning with ski bending are shown in Fig. 3.1.

It is important to understand that deflection is not only ruled by the amount of load applied (weight and centrifugal force) but is strongly influenced by the edge angle created while turning. As explained by Nikitin [7] and depicted in Fig. 3.2, the higher the edge angle, the more the ski is capable of bending, otherwise there will not be turning effect but only sliding following the ski radius.

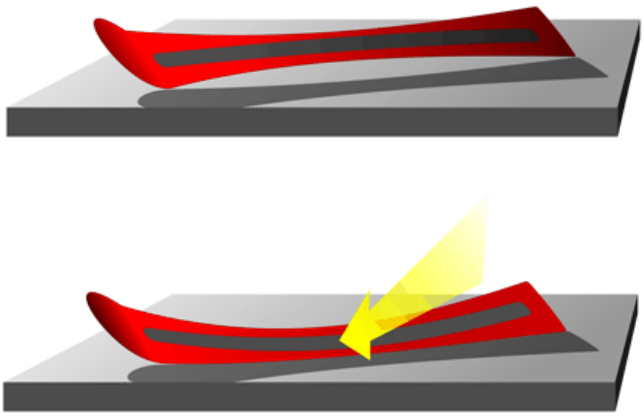

Figure 3.1: Railing and bending during a turn. [7]

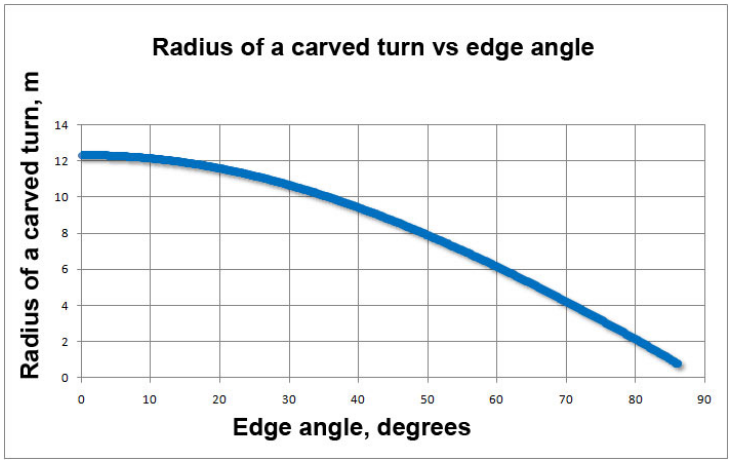

Figure 3.2: Radius of the curve in function of the edge angle. [7]

With more edge angle the flexural behaviour is enhanced and a rebound effect is formed. Due to its stiffness, the ski behaves like a spring, so with bigger deflection the rebound effect will be higher. The latter represents a key aspect during racing, where the athlete aims to be as fast as possible in changing direction.

3.2 Torsion

Twist is more complex to imagine: it is the deformation along the longitudinal axis of the ski. This type of deformation is very rare on straight skies, but it becomes determinant in the behaviour of a parabolic ski because, when it is inclined on the snow, the waist [1] does not touch the below surface.

If the ski was perfectly stiff on the longitudinal axis (torsional stiffness infinite), the ski would make the same angle with the snow in all points (at heel, shoe and tip). In this case the only deformation observed is deflection due to bending.

[1] Waist or width underfoot is the width of the ski beneath the boot

In a more general case, since the ski always has a certain torsional flexibility, its angle with the snow is always greater at skate level than at the tip and tail. In fact, in proximity of the bindings, skier is able to impose a certain angle while at tip and tail the angle results smaller under the snow reaction force, that pushes on edge twisting the ski. This tendency is highlighted in Fig. 3.3.

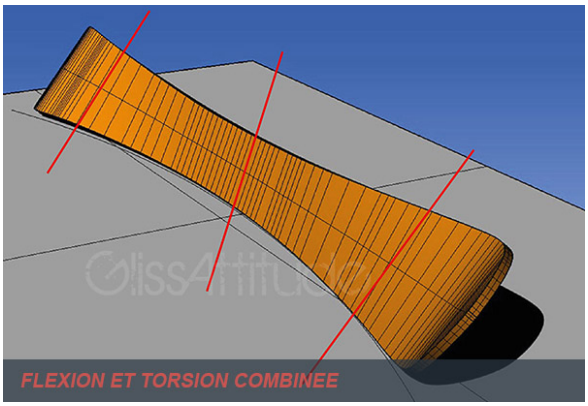

Figure 3.3: Torsion during turn. [8]

On the basis of this observation, a ski with high torsional stiffness will offer little twist when cornering, a grip distributed over the entire edge, precise cornering and high speed stability. Otherwise, a flexible ski in torsion will offer poor grip on hard snow or ice, inaccuracy when cornering and a lack of stability at high speed.

3.3 Remarks

It is now reasonable to investigate the importance of torsion and bending during skiing action and which combination of stiffness is the best one, (depending on different conditions). According to De Gobbi and Petrone [9], during the execution of a turn, bending action is the most relevant, if compared to torsion, especially for the inner ski, that is approximatively only bent thanks to the better control achievable that reduces the difference among tip, tow and middle gradients.

Concerning the global stiffness and the role of ski as connection between the athlete and snow, it can be associated to car suspensions connecting car chassis with the tyres and so the road. In fact, suspensions could be not necessary if the road was flat, but due to the bumps, potholes and its intrinsic roughness, the suspension appears fundamental in order to follow the road, giving comfort and ensuring driveability. The same reasoning can be extended to ski. The Tab. 3.1 proposes preferable stiffness combinations based on the author direct experience and on discussions of the main skiers blog.

Obviously as reported by Nachbauer et al. [10], it is not possible to decouple flexural and torsional stiffness. In fact, high correlation coefficients with a nearly zero level of significance has been found. These are generic considerations, that for ski touring become more complex due to weight requirements to be satisfied. Generically a low bending stiffness is required while skiing on irregular paths (such

as on choppy snow [2]) or for surfing in powder [3]. On the other hand, during ski racing, a high bending stiffness is mandatory, to enhance a good control in turning.

Table 3.1: Comparison of bending and torsional stiffness

Discipline	Bending Stiffness	Torsional Stiffness
Freestyle	SOFT	SOFT
Ski touring	HIGH	MEDIUM
Alpine ski	HIGH	HIGH

Stiffness and vibrations can be connected by a simple formula that states:

$$\omega_n = \left(\frac{n\pi}{L}\right)^2 \sqrt{\frac{EJ}{\rho A}} \tag{3.1}$$

ω_n represents the natural frequency of n-D.o.F, that is the system frequency at which system is disrupted from its equilibrium condition and starts to swing. As consequence, higher values of natural frequency correspond to lower static deflection. But, depending on the frequency of load application Ω, the ski dynamic behaviour can be increased or decreased.

The importance of ski flexibility is fully explored by many of the major brands which try to minimize as much as possible the effect of ski vibrations developing new technology. Here the most interesting are presented:

- Atomic with *Servotec*
- Volkl with *UVO*[4]
- Head with *ECM*[5]

Servotec is based on the presence of a rod under tension that compresses the elastomer at its end positioned below front binding. The whole ski appears to be in a pre-stressed position, so as ski bends into a turn, compression in the elastomer is relaxed. Then, once the turn is finished, the rod returns in its original positions and vibrations are strongly reduced thanks to elastomer (which acts like a damper). This makes steering lighter, quicker and reduces the global instability of ski, especially at high speeds. Fig. 3.4 represents Servotec mounted on the ski, focusing on the elastomer position.

As suggests by the name itself, *UVO 3D*, is a device acting in the three directions. This is possible thanks to the presence of a spring, which reduces the most critical vibrations along the vertical axis, and the use of an elastomer absorbing vibrations in the same plane of the ski. In Fig. 3.5, *UVO 3D* position and its main components are depicted.

ECM is the only existent technology in the ski field, that acts on vibration reduction through electricity. In particular, the presence of piezoelectric has the function to convert kinetic energy into electric energy. The generated current passes

[2]Opposite of groomed track, it is a late afternoon track condition characterized by snowdrifts
[3]Sweetest type of snow thanks to the low moisture content, it is the freshly fallen snow
[4]Ultimate Vibration Object
[5]Energy Management Circuit

through resistor where the stored energy is dissipated. Fig. 3.6 shows the technology as presented by the company.

(a) *Servotec* **(b)** *Elastomer detail*

Figure 3.4: Atomic Servotec technology. [11]

(a) *UVO 3D location* **(b)** *UVO 3D Assembly*

Figure 3.5: Volkl UVO 3D. [12]

Figure 3.6: Energy Management Circuit. [13]

It is evident the attention given to this aspect in alpine skiing. In the same way it is mandatory in ski touring, but, due to the lower weight involved, it becomes necessary to give more importance to the choice of materials without adding devices and, therefore, weight.

For this reason, it is interesting to focus briefly on the damping vibrations property of fiber composites. The damping property of a material represents its capacity to reduce the transmission of vibrations caused by mechanical disturbances. The measure of damping is its damping factor η. An high value of η is preferable to reduce the resonance amplitude. Fiber reinforced composites have a higher damping factor than metals, but it is worth noticing that this tendency is influenced by

several factors, such as fiber and resin types, fiber orientation angle and stacking sequence. Tab. 3.2 proposes a comparison of some materials typical damping factors.

Table 3.2: Representative damping factors of various polymeric laminates [4]

Material	Fiber Orientation	Modulus ($10^6 psi$)	Damping Factor η
Mild steel	-	28	0.0017
6061 Al alloy	-	10	0.0009
E-glass-epoxy	0°	5.1	0.0070
Boron-epoxy	0°	26.8	0.0067
Carbon-epoxy	0°	27.4	0.0157
	22.5°	4.7	0.0164
	90°	1.0	0.0319
	$[0/22.5/45/90]_s$	10.0	0.0201

3.4 Conclusions

The understanding of the actions, to which ski is subject during skiing, allows to understand which aspect must be investigated in order to obtain the desired behaviour. All the decisions in terms of material affects the mechanical nature of a ski and so its performances. Each discipline needs specific requirements and the ski manufacturer must be able to satisfy those aspects by introducing new elements or by changing the construction developing new solutions.

Chapter 4

Finite Element Method

[1] FEM[2] (Finite Element Method) is a mathematical tool that allows to predict the physical change of a component under mechanical, thermal and electromagnetic conditions by subdividing the object region into finite elements. It can be defined as a method of computing the whole.

The main motives to use this type of simulation process are to reduce product development lead time and cost, improving the quality and matching the desired performance. In addition, it becomes crucial when testing is not feasible.

4.1 Short remarks

The basic concept of FEM is the discretization of a continuum object that has almost unlimited degrees of freedom. Once divided in small finite elements the D.o.F.[3] become finite. Each element is composed by nodes. Depending on the element complexity the number of nodes will be different and so the total number of D.o.F.

The software theory is based on element equilibrium

$$[R]_e = [K]_e \cdot [D]_e \tag{4.1}$$

where D is the vector of nodal displacement, K represents the stiffness matrix dependent on Young's Modulus and Poisson's coefficient and R is the vector of known loads.

The assembly of discrete elements equations gives the set of equations for the complete structure. Being an approximation of the real model, three main sources of error may be present in FEM solution:

1. *discretization errors*: they result from transforming the physical system (continuum) into a finite element model,

2. *formulation error*: they regards wrong element selection that cannot represent the physical problem for geometric or mathematical reason,

[1] The main literature reference for this chapter is: *Finite element modeling for stress analysis* [14].

[2] Finite-element Method

[3] Degree of freedom

3. *numerical error*: they occur independently from users and it involves truncation errors and round off errors.

4.2 Elements and nodes

Finite elements resemble fragments of the structure, in which nodes appear on element boundaries, serving as connectors that hold the elements together. In Fig. 4.1, a mix of elements are presented (both triangular and quadrilateral), with nodes indicated by dots. Considering two elements sharing the same node, they have the same displacement components at node. Thus, elements can have nodes only at corners or nodes on sides as well.

It is not only a sawing and reconnecting operation, because this can produce a weak and unrepresentative model due to the strain concentrations, sliding of elements on one another and even gaps. Indeed, to enable the convergence, each element is restricted to its mode deformation.

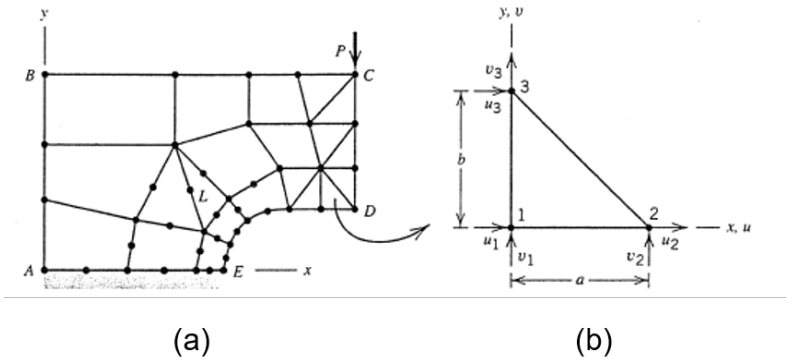

Figure 4.1: (a) A flat bracket modelled by several element types (b) One of the elements, a "constant strain triangle". [15]

4.2.1 Plane elements

By definition, a plane body is flat and characterized by a constant thickness. Based on the assumption of plane stress or plane strain, it can represent correctly thin or thick plate elements.

Plane stress is a condition characterized by $\sigma_z = \tau_{yz} = \tau_{zx} = 0$, i.e. all the stresses out of plane are null, while stresses acting in the plane of the plate are called membrane stresses. Strains in all directions are different from zero, so the thickness is free to increase or decrease in response to stresses in xy plane. As the thickness of a plane body increases, from much less to greater than in-plane conditions of the body, there is a transition of behaviour from plane stress toward plane strain.

Plane strain is a state of strain in which normal strain and shear strains directed perpendicular to the plane of the body are assumed to be zero. Assuming xy plane as body plane, the only nonzero strains are: ε_x, ε_y and γ_{xy}. The value of the third

principal stress guarantees the deformation perpendicular to plane of the body to be zero and prevents thickness changes.

Constant strain triangles

CST[4] is the earliest and simplest finite element. In terms of generalized coordinates β_i its displacement field is:

$$u = \beta_1 + \beta_2 x + \beta_3 y \tag{4.2a}$$

$$v = \beta_4 + \beta_5 x + \beta_6 y \tag{4.2b}$$

$$\varepsilon_x = \beta_2 \quad \varepsilon_y = \beta_6 \quad \gamma_{xy} = \beta_3 + \beta_5 \tag{4.2c}$$

So strains are constant, hence the name constant strain triangle, while the displacement field is linear.

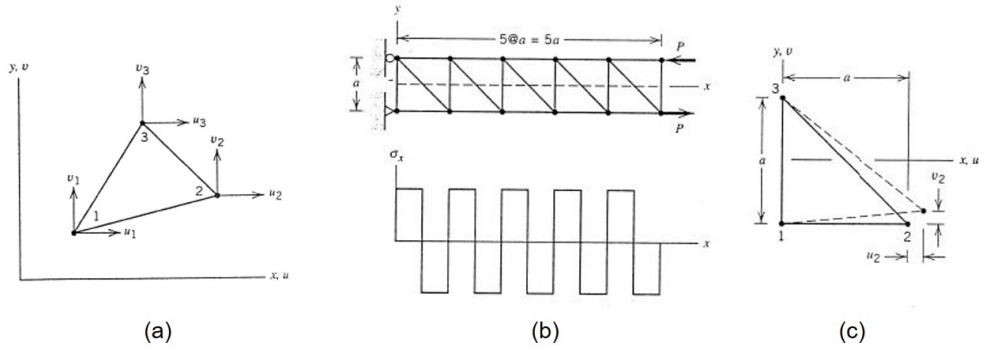

Figure 4.2: (a) Constant strain triangle (b) Stress σ_x along the axis in a beam modelled by CST and loaded in pure bending (c) Deformation of the lowest-left in the model. [14]

This element acts well in case of little stress gradient. However, as it can be seen in Fig. 4.2, it is not the right choice considering pure bending, as the model will display σ_x as a square wave pattern. In addition, spurious shear effects are formed. Although, with a small mesh the result can refined.

Linear strain triangles

LST[5] has midside nodes in addition to vertex nodes

$$u = \beta_1 + \beta_2 x + \beta_3 y + \beta_4 x^2 + \beta_5 xy + \beta_6 y^2 \tag{4.3a}$$

$$v = \beta_7 + \beta_8 x + \beta_9 y + \beta_{10} x^2 + \beta_{11} xy + \beta_{12} y^2 \tag{4.3b}$$

$$\varepsilon_x = \beta_2 + 2\beta_4 x + \beta_5 y \quad \varepsilon_y = \beta_9 + \beta_{11} x + 2\beta_{12} y \tag{4.3c}$$

$$\gamma_{xy} = (\beta_3 + \beta_8) + (\beta_5 + 2\beta_{10})x + (2\beta_6 + \beta_{11})y \tag{4.3d}$$

The displacement field is quadratic in x and y. Therefore, the strain field is able to vary linearly with x and y within the element, so the name linear strain triangles. This feature solves the problem of modelling correctly the bending phenomena as depicted in Fig. 4.3.

[4]Constant Strain Triangle
[5]Linear Strain Triangle

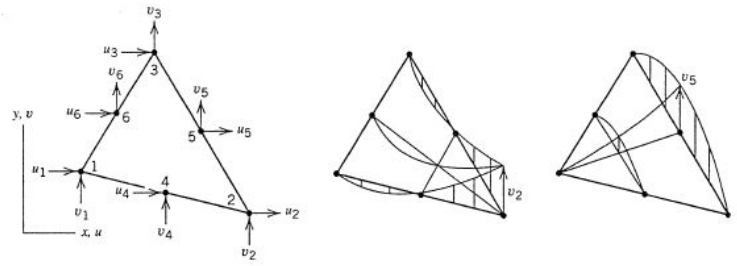

Figure 4.3: Linear strain triangle and deformation mode. [14]

Bilinear quadrilateral

Q4[6] is a quadrilateral that has four nodes for a total of 8 D.o.F. Displacement in terms of β is:

$$u = \beta_1 + \beta_2 x + \beta_3 y + \beta_4 xy \tag{4.4a}$$

$$v = \beta_5 + \beta_6 x + \beta_7 y + \beta_8 xy \tag{4.4b}$$

$$\varepsilon_x = \beta_2 + \beta_3 y \quad \varepsilon_y = \beta_7 + \beta_8 x \tag{4.4c}$$

$$\gamma_{xy} = (\beta_3 + \beta_6) + \beta_4 x + \beta_8 y \tag{4.4d}$$

The name bilinear is related to the expressions of u and v, as they are the product of two linear polynomials.

It must be noted the independence of ε_x from x and ε_y from y. Despite its ability to represent a strain ε_x which varies with y, it cannot model exactly a cantilever beam under transverse tip force where axial strain varies linearly with x. Considering a cantilever beam loaded in pure bending, as presented in Fig. 4.4, the theory says that γ_{xy} is absent and plane section remains plane, with top and bottom edges become arcs of practically the same curvature. What happens in Q4 element is that a rotation of lateral edges occurs, while top and bottom edges remain straight. As a consequence 90° angle is no more maintained and a shear strain appears everywhere except along y axis.

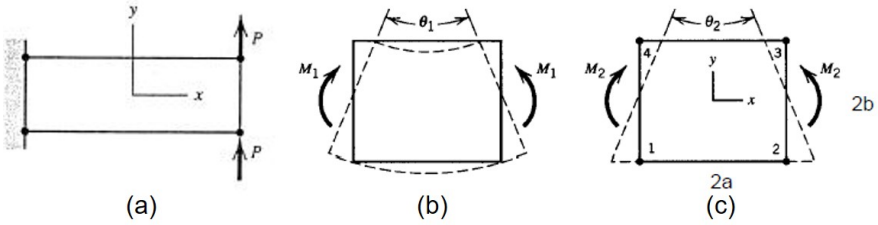

Figure 4.4: (a) A one-element cantilever beam under transverse tip loading (b) Correct deformation under bending (c) Deformation of the bilinear quadrilateral under bending loading. [14]

Physically, this causes an overestimation of the structure stiffness due to a spurious shear stress. Bending moments M_1 and M_2 are necessary to make vertical sides of the box and keep ϑ_1 equal to ϑ_2. This condition is satisfied for:

[6] Bilinear quadrilateral

$$M_2 = \frac{1}{1+\nu}\left(\frac{1}{1-\nu} + \frac{1}{2}\left(\frac{a}{b}\right)^2\right) M_1 \tag{4.5}$$

In which a and b are the dimensions of the rectangle. If $\frac{a}{b}$ increases without limit, also M_2, which means infinite stiffness traduced as locking.

This last condition can be avoided by reducing the aspect ratio, even if this will not solve the general structure over stiffness.

Improved bilinear quadrilateral

The Q6[7] has the function to solve the over stiffness in bending of Q4, as depicted in Fig. 4.5, in which Q6 top and bottom edges deform in a curved way.

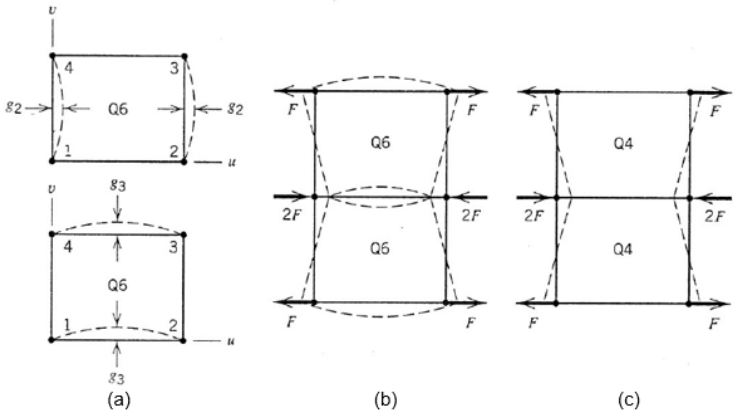

Figure 4.5: (a) Displacement modes $u = (1-\eta^2)g_2$ and $v = (1-\varepsilon^2)g_3$ in the Q6 element (b) Incompatibility between adjacent Q6 elements (c) No incompatibility between adjacent Q4 elements. [14]

Displacements and shear are an evolution of Q4, with two more added fictitious D.o.F.

$$u = \sum_1^4 N_i u_i + (1-\xi^2)g_1 + (1-\eta^2)g_2 \tag{4.6a}$$

$$v = \sum_1^4 N_i v_i + (1-\xi^2)g_3 + (1-\eta^2)g_4 \tag{4.6b}$$

$$\gamma_{xy} = \sum_1^4 \frac{\partial N_i}{\partial y} u_i + \sum_1^4 \frac{\partial N_i}{\partial x} v_i - \frac{2y}{b^2} g_2 - \frac{2x}{a^2} g_3 \tag{4.6c}$$

With $\xi = \frac{x}{a}$ and $\eta = \frac{y}{b}$

In case of rectangular elements it can represent pure bending with additional shear stresses that vanishes. This kind of elements is also called *Incompatible*.

[7] Improved bilinear quadrilateral

Quadratic quadrilateral

The Q8[8] element has a total number of 16 D.o.F. that corresponds to 2 D.o.F. for each of the eight node. In terms of generalized coordinates β_i its displacement field is

$$u = \beta_1 + \beta_2 x + \beta_3 y + \beta_4 x^2 + \beta_5 xy + \beta_6 y^2 + \beta_7 x^2 y + \beta_8 xy^2 \tag{4.7a}$$

$$v = \beta_9 + \beta_{10} x + \beta_{11} y + \beta_{12} x^2 + \beta_{13} xy + \beta_{14} y^2 + \beta_{15} x^2 y + \beta_{16} xy^2 \tag{4.7b}$$

$$\varepsilon_x = \beta_2 + 2\beta_4 x + \beta_5 y + 2\beta_7 xy + \beta_8 y^2 \tag{4.7c}$$

$$\varepsilon_y = \beta_{11} + \beta_{13} y + 2\beta_{14} y + 2\beta_{15} xy + \beta_{16} y^2 \tag{4.7d}$$

$$\gamma_{xy} = (\beta_3 + 10) + (\beta_5 + 2\beta_{12})x + (2\beta_6 + \beta_{13})y + \beta_7 x^2 + 2(\beta_8 + \beta_{15})xy + \beta_{16} y^2 \tag{4.7e}$$

This kind of element can represent exactly all states of constant strain and state of pure bending, if it is rectangular. Non rectangular shapes are permitted too.

4.2.2 Elements for 3D solids

As alternative, modelling can be based on solids, this means that the elements are effectively 3D parts. The solid (or continuum) elements can be used for linear analysis and for complex nonlinear analyses involving contact, plasticity and large deformations.

The term 3D solid means a three dimensional solid with no restrictions regarding shape, loading, material properties and boundary conditions. This implies the analysis of all six possible stresses, three normal and three shear and of all three possible displacements along the directions. Typically, as shown in Fig. 4.6, finite elements have tetrahedral and hexaedral shape with three D.o.F. for each node.

For what concerns the strain-displacement relations, by assuming $u = u(x, y, z)$, $v = v(x, y, z)$ and $w = w(x, y, z)$ as displacements components of an arbitrary material point in x, y and z directions, the strain and displacement gradients are related by these equations:

$$\varepsilon_x = \frac{\partial u}{\partial x} \quad \gamma_{xy} = \frac{\partial u}{\partial y} + \frac{\partial v}{\partial x} \tag{4.8a}$$

$$\varepsilon_y = \frac{\partial v}{\partial y} \quad \gamma_{yz} = \frac{\partial v}{\partial z} + \frac{\partial w}{\partial y} \tag{4.8b}$$

$$\varepsilon_z = \frac{\partial w}{\partial z} \quad \gamma_{zx} = \frac{\partial w}{\partial x} + \frac{\partial u}{\partial z} \tag{4.8c}$$

Usually, solid elements are simply the direct extensions of plane elements, consisting in the addition of another coordinate (or displacement) component.

[8] Quadratic quadrilateral

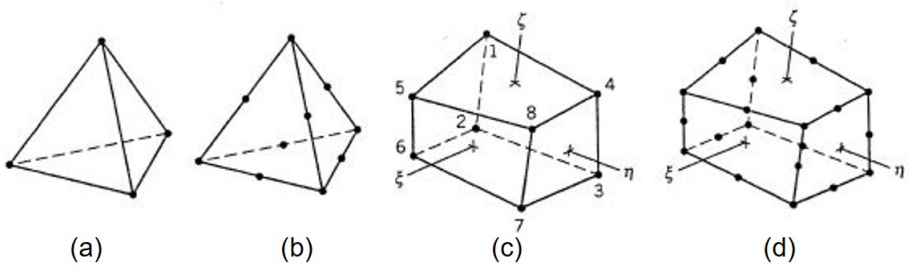

Figure 4.6: (a) Constant strain tethraedron (b) Linear strain tethraedron (c) Trilinear hexaedron (d) Quadratic Hexaedron. [14]

Constant strain tethraedron

Characterized by three translational D.o.F. at each of its four nodes, for a total of 12 D.o.F. (Fig. 4.6) . Displacement field is:

$$u = \beta_1 + \beta_2 x + \beta_3 y + \beta_4 z \tag{4.9a}$$
$$v = \beta_5 + \beta_6 x + \beta_7 y + \beta_8 z \tag{4.9b}$$
$$w = \beta_9 + \beta_{10} x + \beta_{11} y + \beta_{12} z \tag{4.9c}$$

Its main limitation is that it can be used only in the case of constant strains over the span of an element. It is not appropriate when modelling bending or twisting if the axis of bending or twisting intersects the element or is close to it.

Linear strain tethraedron

The total number of D.o.F. is 30, three D.o.F. for each of the ten nodes (Fig. 4.6). The strain is linear in the coordinates and this allows a correct representation of the pure bending. The undeformed elements can be straight or curved depending on the coordinates of the edge nodes.

Trilinear hexahedron

It is also known as eight-node brick (Fig. 4.6). The displacement field is:

$$u = \beta_1 + \beta_2 x + \beta_3 y + \beta_4 z + \beta_5 xy + \beta_6 yz + \beta_7 zx + \beta_8 xyz \tag{4.10a}$$
$$v = \beta_9 + \beta_{10} x + \beta_{11} y + \beta_{12} z + \beta_{13} xy + \beta_{14} yz + \beta_{15} zx + \beta_{16} xyz \tag{4.10b}$$
$$w = \beta_{17} + \beta_{18} x + \beta_{19} y + \beta_{20} z + \beta_{21} xy + \beta_{22} yz + \beta_{23} zx + \beta_{24} xyz \tag{4.10c}$$

All linear modes are considered, also some quadratic modes (x^2, y^2, z^2 are missing) and one of the cubic modes (xyz). As the bilinear quadrilateral, it cannot model beam action well because its sides remain straight as the elemet deforms. This produces shear locking effect as already explained for bilinear quadrilateral (Subsection 4.2.1).

Quadratic hexahedron

Number of nodes is 20, for a total of 60 D.o.F. (Fig. 4.6). As the linear strain tetrahedron, edges of underformed elements can be straight or curved. If the element

is rectangular linear strain fields are modelled exactly. There is the possibility to have a near instability. This problem can be solved by changing Gauss integration rule.

4.2.3 Shell element

Modelling can be based on shell elements in order to simplify the structure, thus decreasing number of nodes and, subsequentially the computational time. With this part topology, the main concept is to consider the elements as 2D, so they can be totally described in one plane (xy). As consequence, the constants needed to describe each material are four: E_x, E_y, G_{xy}, ν_{xy}. To understand the cases in which shell elements can be applied, it is important to consider their general characteristics and the reason behind this element choice.

Shell elements are used to simulate the behaviour of bodies with a well defined shape. In particular, the ratio between thickness and its characteristic length must be lower than 1/20.

Shell elements can be seen as a combination of membrane and bending elements. Thus, a simple triangular shell element can be obtained by combining the plane stress triangle (Fig. 4.2) and plate bending triangle. The resulting element is flat and has five (or six) D.o.F. per node, depending on the presence of shell normal rotation ϑ_{zi} at node i in the plane stress element. A quadrilateral shell element can be produced by combining quadrilateral plane and plate elements. Attention to possible warping must be considered due to nodes non coplanarity.

A flat element has the advantage to introduce simplicity of the element formulation, both in terms of geometry description and capability to represent rigid body motion without strain. Disadvantages include the difficulty while representing a smoothly curved shell surface by flat or slightly warped facets, so that fold lines are present where elements meet.

In shell, discretization error is associated due to the lack of coupling between membrane and bending actions. For this reason, low mesh is preferred. Curved elements can be used, but the complexity in terms of geometry arises. Membrane and bending actions are coupled, so it is difficult to avoid a great over stiffness in bending because the membrane stiffness is far greater than bending one if the shell is thin. Isoparametric shell elements occupy a middle ground between flat elements and curved elements based on shell theory. Starting from the 3D solid shown in Fig. 4.7, the element can be modelled as a shell if thickness is small in comparison with other dimensions. Number of nodes is reduced from 20 to 8.

In the shell nor node a nor c are present, so the displacements at a and c are expressed as function of node b.

$$u_a = u_b - \frac{t}{2}\vartheta_{yb} \qquad u_c = u_b + \frac{t}{2}\vartheta_{yb} \tag{4.11a}$$

$$v_a = v_b + \frac{t}{2}\vartheta_{xb} \qquad v_c = u_b - \frac{t}{2}\vartheta_{xb} \tag{4.11b}$$

$$w_a = w_b \qquad w_c = w_b \tag{4.11c}$$

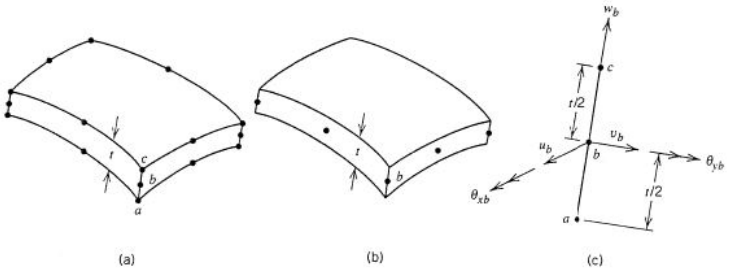

Figure 4.7: (a) A 20-node isoparametric solid element (b) Reduction to an 8-node shell element (c) The D.o.F. at typical node *b*. [14]

With the above relations, for all thickness direction lines of nodes, shape functions are transformed to operate on the three translations and on the two rotations at each node of the 8-node element.

A reduced or selective integration scheme may be used to avoid transverse shear and/or membrane stiffness. It is usually more reliable in terms of convergence. As shown in Fig. 4.8, shell elements are divided into two categories.

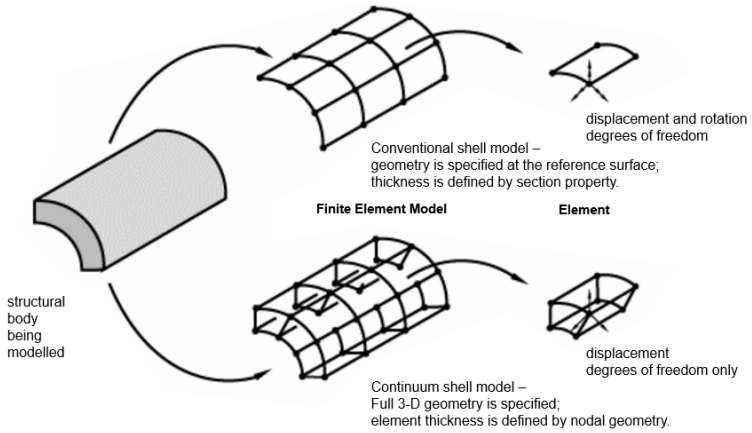

Figure 4.8: Conventional and continuum shell elements. [15]

1. *Conventional shell elements*

   They are the most used and the ones commonly addressed speaking about "shell". Conventional shell elements are classical 2D elements, whose thickness is defined through definition of the section property. It consists in discretization by defining the geometry at a reference surface. Conventional shell elements have displacement and rotational degrees of freedom.

2. *Continuum shell elements*

   In contrast, continuum shell elements discretize an entire three-dimensional body. The thickness is determined from element nodal geometry. Continuum shell elements have only displacement degrees of freedom. They can be seen as a hybrid solution between solid for the appearance and conventional shell element for its kinematic and constitutive behaviour. Unlike conventional

shell, continuum shell element allows higher thickness-length ratio and it is more suitable to reproduce contact and boundary conditions coherent with the real case. Being a more complex structure compared to the conventional one in terms of number of nodes, the computation effort are higher and the analysis result less fluent in terms of convergence.

4.3 Conclusions

In this chapter the potentiality of Finite Element Simulation were considered. It was briefly presented the theory behind each analysis, focusing especially on the description of the element types, considering their characteristics and explaining how the simulation can be influenced by a specific element choice.

Chapter 5

Ski Model- SkiTrab Freedom 90

Chapter 1 introduces the general technical requirements of a ski. This chapter shows the ski used as reference in this work. Materials, technologies and geometry are analysed in order to understand exactly its behaviour to be able to predict its response on snow.

The ski model, displayed in Fig. 5.1, is a SkiTrab Freedom 90 realized by SkiTrab. From a famous ski magazine [16], it is described as an Adventure Ski perfect in terms of reliability, weight and handling, giving a good response both in uphill and downhill phase.

Figure 5.1: Model Freedom 90 [17]

5.1 Geometry

Tab. 5.1 lists the main ski characteristics.

Table 5.1: SkiTrab Freedom 90 technical details [16]

Size	171 cm
Weight	1370 g
Sidecut	125/123/90/112 mm
Radius	19.5 m

It is interesting to concentrate on sidecut dimension that identifies the width of ski from tip to tail, where 90 represents the central part dimension where bindings are positioned.

Higher length means higher radius that makes the ski suitable for tracks with a lower number of turns, while shorter ski means a ski easier to handle in turning, that is preferred for slalom races. No indications about rocker are present, in fact, the ski does not show rocker nor in tip nor in tail, making the ski more suitable for the use on hard snow rather than on powder.

The camber is another important characteristic especially for ski handling. The camber value is 5 mm, this ensures a proper bending effect and so an adequate contact with the snow, thus properly directing the ski. For this reason it results to be "funny" also for downhill phase without loosing its nature of ski touring.

5.2 Materials and technology

Fig. 5.2 shows the section given by the company. It is interesting to notice the presence of nine layers with specific shape and thickness.

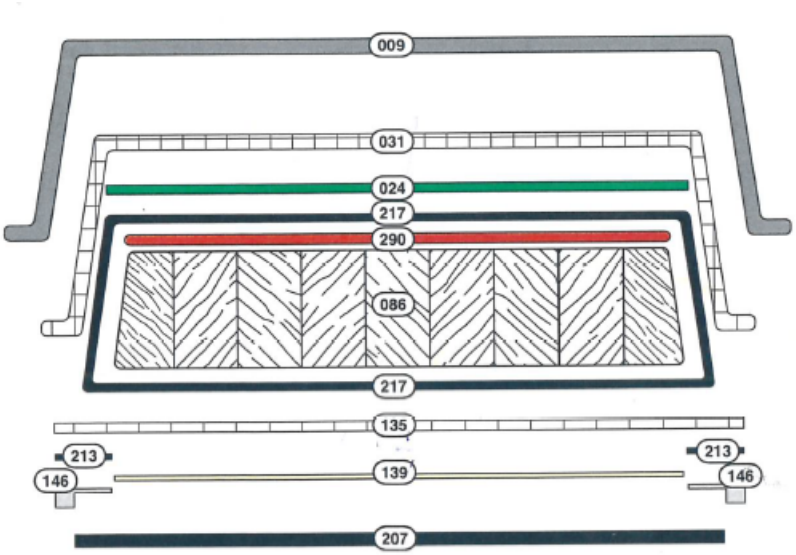

Figure 5.2: SkiTrab Freedom90 section. [17]

The above figure adds further informations referring to construction technique, that is an example of Cap construction (Chapter 1), with no ABS sidewalls that run all over or partial length.

The properties of the materials composing the ski were already partially studied by Concli and Fraccaroli [18] using DIC[1] procedure. The availability of materials to realize specimens, together with the concrete possibility to realize composite specimen as well as wood specimen, lead to the decision to test them. This represents an important opportunity in order to validate the use of TexGen[2] software to simulate composites to be used for this specific application.

Table 5.2 shows the material of each different ski layer and the method in which these properties are obtained.

[1]Digital Image Correlation
[2]Open source software for modelling the geometry of textile structures

Table 5.2: SkiTrab Freedom 90 materials

Material	Type	
9	Nylon	
31	Textile glass fibers	
24	Glass fiber composite	
217	Basalt glass fibers	LiWood Core
290	Glass fiber composite	
86	Ash - Paulownia	
217	Basalt glass fibers	
135	Textile glass fibers	
139	ABS	
146	Steel	
207	Polyetilene	

5.2.1 LiWood Core

The ski manufacturer describes its Liwood core (Fig. 5.3) as *"A new light wood core reinforced with a fiberglass box wrapping around the skies provides light and high performance skies with durability and resistance. Wood is the most used raw material in ski production. For years designers have sought after a wood that is lightweight yet durable and strong, yet this goes against nature. A lightweight wood core needs to be supported by production processes and to be mixed with other types of wood to improve its strength; above all it must be wrapped by composite materials which give it torsional rigidity and durability".*

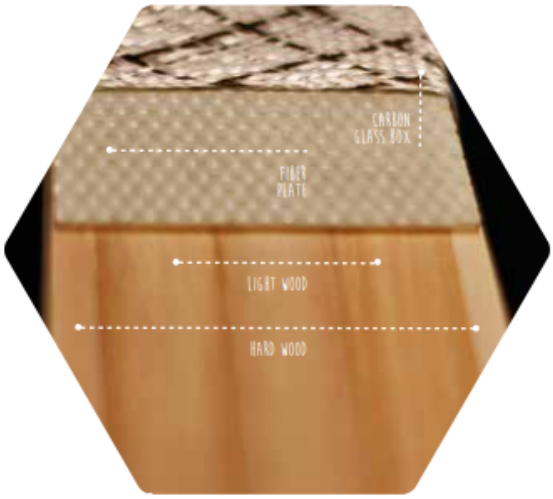

Figure 5.3: Liwood core. [17]

From an engineering point of view, the presence of this fiber box obviously enhances the torsional properties of the ski. This is evident considering the presence of basalt and glass fibers twisted together forming 45°. The idea to combine different fibers comes from the automotive world, as it allows reinforcement along the main load path without an excessive cost increasing. The combination of soft wood at

the center and hard at the extremes is chosen to strength the ski in proximity of the edge that is subjected to higher loads due to the combination of weight and centrifugal force when approaching a turn.

This technology does not simply provide optimum results in terms of torsional rigidity but also allows to not increase strongly ski longitudinal stiffness, that is one of the most critical issues of the design process.

Fiber box

Fiber box is the name given by the ski manufacturer company to the cage. It has the function to embody the fiber plate and the combination of woods. Having available a sample given by the company, it is interesting to notice the combination of such filaments and their orientation. This textile combined with a certain amount of epoxy resin gives to cage the desired mechanical properties.

Being not able to test the specimen, because the low density of fibers combination does not allow to obtain a rigid material suitable to be tested, its behaviour has been simulated with Texgen software. This software enables to reproduce the shape of fibers and how they are arranged together.

Through the modelling of a micromechanical unit cell of 4-Harness satin weave fabric textile composite, an estimation of properties of the whole material is performed based on the assumption that the unit cell is able to enclose the periodic repeated pattern in fabric weave. As reported by Wu et al. [19], periodic boundary conditions are commonly applied in molecular dynamics, dislocation dynamics and materials modelling to eliminate the existence of surface and avoid huge amount large size molecules of simulation box. The idea is to form an infinite lattice system by repeating the unit cell through space. The unit cell geometry of the basalt glass composite is shown in Tab 5.3 and Tab 5.4.

Table 5.3: Fiber Box unit cell size

Length $[mm]$	Width $[mm]$	Thickness $[mm]$	Volume $[mm^3]$
9.65	9.65	0.5	46.56

Table 5.4: Input data for yarn modeling - Fiber box

Yarn Spacing $[mm]$	Yarn width $[mm]$	Fabric thickness $[mm]$	N° of Warp Yarns	N° of Weft Yarns
2.4125	1.35	0.4	04	04

Giving to the software these input data, the unit cell is created as depicted in Fig. 5.4

The fiber properties, expressed in Tab.5.5, are taken from literature in particular glass fibers are assumed to be isotropic as reported by Mounier et al. [20] in which the value of longitudinal and transverse modulus were found to be similar. Also basalt fibers can be assumed as isotropic according to Valentino et al. [21].

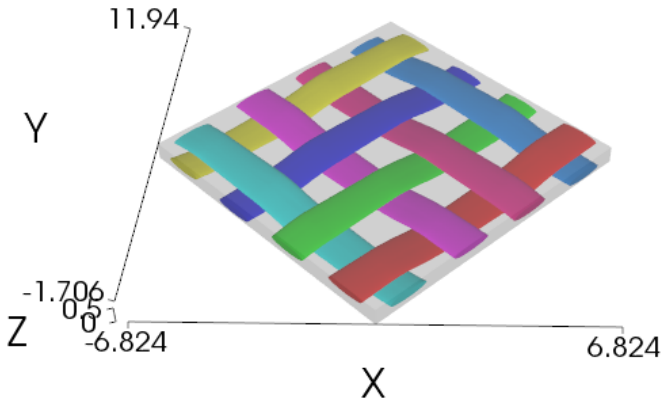

Figure 5.4: Unit Cell of the basalt glass composite.

Table 5.5: Fiberglass and basalt mechanical properties

Material	E_x [GPa]	ν_{xy} [-]
E glass	72.4	0.2
Basalt	89	0.26

The analysis has been performed in an automatic manner by producing an .inp file that is analysed then in Abaqus ©[3], giving the final composite mechanical properties (Tab. 5.6). In fact in the submitted file, periodic boundary conditions as well as loads are already indicated.

Table 5.6: Basalt-glass composite mechanical properties

Material	E_x [GPa]	E_y [GPa]	E_z [GPa]	G_{xy} [GPa]	G_{yz} [GPa]	G_{zx} [GPa]	ν_{xy} [-]	ν_{xz} [-]	ν_{yz} [-]
Basalt-glass composite	11.15	5.36	11.16	6.6	1.67	1.66	0.38	0.23	0.23

The accuracy of TexGen simulation is verified with tests in Section 5.2.2.

Wood core

Concerning the real core of the ski, analysis are based on reasonable assumptions. As there is not an exact definition of the woods employed, starting from the data available on the company website, it is appropriate to assume that the hard wood is ash while the soft wood could be paulownia, one of the lightest wood available. Ash is positioned at the extremes to ensure a stronger behaviour, while paulownia is certainly chosen for its low density, without decreasing strongly the elastic modulus as it could be if balsa wood was selected. From what concerns ash, the data are

[3]Software suite for finite element analysis and computer-aided engineering

taken from literature, according to Niemz et al. [22] and focusing on dry ash, that has a relative humidity of 12%.

While for paulownia tree, being a relative unknown wood, the data available in literature were not enough to characterize it at least in longitudinal plane xy. For this reason a tensile test has been performed on properly cut specimen as suggested by ASTM 1037. The specimens are obtained in longitudinal and tangential direction (Figure 5.5), and the test aims to find E_l and E_t, no Poisson's ratio can be established due to the impossibility to perform a more specific test using DIC procedure or mounting specific extensometers.

Testing procedure consists in two phases:

- Preparation of the specimen
- Test of the specimen

Preparation of the specimen

The specimens are obtained cutting a table of Paulownia wood using a CNC wood machine. A total number of six specimens, three for longitudinal and three for tangential directions are realized. Their dimension are the ones suggested by standard.

In Fig. 5.5 examples of longitudinal and transversal specimen are shown.

Figure 5.5: Longitudinal and trasnversal wood sample

Specimen thickness was initially 18 mm, but due to the impossibility to perform a tensile test on a specimen with this kind of toughness using hydraulic machine, the choice was to reduce this value in order to allow the use of mechanical grips. This permits to hold the specimen without an excessive deformations from the clamping force.

Test of the specimen

Following the standard suggestions, after placing the specimen in the machine, speed has been set to 4 mm/min. Three test for longitudinal and transversal directions have been performed on Polimi machines. Fig. 5.6 represents wood testing.

Figure 5.6: Tensile test.

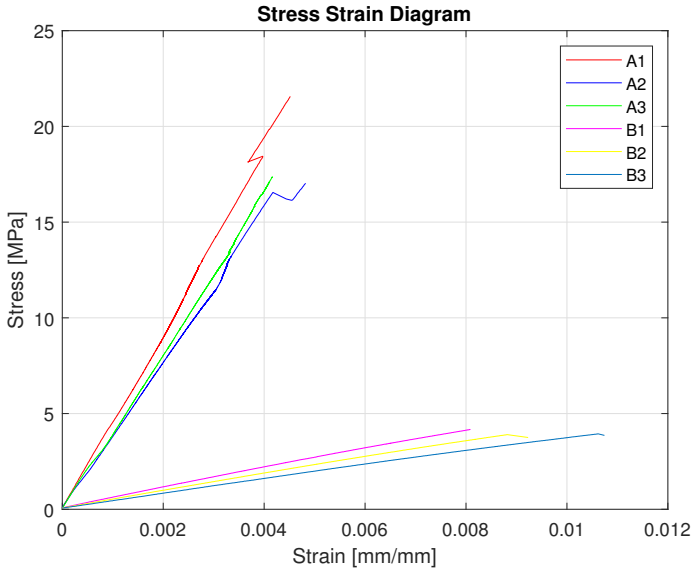

Figure 5.7: Stress strain diagram of Paulownia wood

Table 5.7: Paulownia wood Young Modulus

Specimen	Young's Modulus [MPa]		
	Max	Min	Avg
A	4660	3844	4213
B	538	390	462

In Fig. 5.7 and Tab.5.7 differences in terms of elastic modulus between longitudinal and tangential specimens can be observed. This is an expected behaviour because wood is a natural element composed by grains and fibers aligned randomly, so, depending on the cut region, fibers will enhance or reduce elasticity and in general resistance of the sample. In addition they show a brittle behaviour, in fact once reached the yield strength, plasticity implies a crack nucleation that leads to specimen failure. Due to the impossibility to acquire all its mechanical properties, remaining ones have been found comparing properties of other soft wood, taken by Green, Winandy, and Kretschmann [23], similar in terms of density, transversal and longitudinal elastic modulus. Therefore, a complete characterization is obtained (Tab. 5.8).

Table 5.8: Paulownia wood mechanical properties

Material	E_l [MPa]	E_t [MPa]	E_r [MPa]	G_{lt} [MPa]	G_{tr} [MPa]	G_{rl} [MPa]	ν_{lt} [-]	ν_{lr} [-]	ν_{tr} [-]
Paulownia wood	4213	462	529.4	63.2	561.7	561.7	0.34	0.35	0.34

5.2.2 Textile reinforced composites

Textile reinforced composites corresponds to Material 31 (Figure 5.2). It consists in a combination of woven textile and chopped strand mat, so it can be considered a stitched fabric.

Woven textile and CSM are stitched together by polyester wire. The combination, due to the lightness of CSM reinforcement that is only 50 $\frac{g}{m^2}$, has no effects on whole material strength but it gives better permeability during resin application providing additional resistance for what concerns the shear modulus.

Based on this hypothesis, the model ignores the presence of CSM, simulating only woven textile. The simulation is provided using TexGen, already presented in Sec. 5.2.1. Differently from the previous case, in which experimental simulation was not possible due to the particularity of textile structure, this time the experimental part can be afforded especially in order to make a comparison with properties extracted from the software.

The creation of a composite simulating the one in ski is obviously a simplification, because in the real manufacturing process, the resin plays role of glue and reinforcement, so there is not a finite composite as the one created for this comparison. However it is considered as the best solution to extract the mechanical properties, focusing especially on the searching of coherence with TexGen. The comparison consists in two passages:

- Preparation of the specimen
- Test of the specimen

Preparation of the specimen

To prepare the specimen to be tested, the material given by the company has been used, in addition the resin has been selected. Among all the possible resins that can be used, as explained in Chapter 1, the one usually chosen for ski construction is epoxy. It was not possible to use the exact one employed by the company, although from a deep analysis among the ski manufacturers, it was discovered that all the resins used for this application have common values in terms of tensile modulus (2.7-3.2 GPa) and bending modulus (2.4-3 GPa). Tab. 5.9 lists the properties of the selected resin.

Table 5.9: Epoxy properties

Epoxy SX10EVO		
Tensile strength	[MPa]	60-70
Strain at Break	[mm/mm]	3.5-5
Tensile Modulus	[MPa]	2700-3200
Flexural strength	[MPa]	105-120
Flexural Modulus	[MPa]	2400-2900

When developing a composite by lamination, there is one important parameter to control: the resin pot time. This represents the amount of time workability. If limit is exceeded an exothermic reaction starts, resulting in an hard compound impossible to be used. Another key factor is curing time, that is the time needed to dry resin. The curing time, as pot life, are strongly influenced by temperature, so there are specific resin for "cold curing" (at environmental temperature) and for hot curing (heated in oven).

In this specific case, the specimen has been placed on a lamina of aluminium in order to be filled with resin. The aluminium lamina was covered by a releasing film that is fundamental to let the composite, once finished, easy to be removed. It is recommended to dry properly the releasing with a heater to speed up the production process. At this point the resin can be prepared, according to ISO 1268-1 for the preparation of fiber reinforced plastic specimen, the amount of resin depends on this precise formula:

$$m = m_1 \cdot \frac{100 - V_f}{V_f} \cdot K \tag{5.1}$$

where:

- m_1 mass of glass fibers [g]
- V_f fiber volume fraction
- m mass of resin [g]
- K constant representing an increment due to the amount of resin lost via spills and by absorption of rollers.

Knowing the resin amount m needed, from the technical data sheet, it is set the ratio of hardener and resin equal to 0.25.

$$m = 17.3 \cdot \frac{100 - 40}{40} \cdot 1.2 = 31g \tag{5.2}$$

With $m_{hardener} = 7.75\ g$ and $m_{resin} = 31 - 7.75 = 23.25\ g$.

At this point the resin is poured below and above the fiber layer and distributed homogeneously through a spatula.

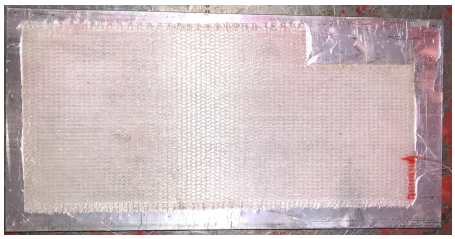

Figure 5.8: Preparation of the composite.

To improve quality and avoid formation of voids a vacuum bag is used. Vacuum bagging (or vacuum bag laminating) is a clamping method that uses atmospheric pressure to hold the adhesive or resin-coated components of a lamination in place until the adhesive cures. When bag is sealed, pressure on the outside and inside of this envelope is equal to atmospheric pressure: approximately 1 atm. As vacuum pump evacuates air from the inside of the envelope, air pressure inside is reduced while air pressure outside remains equal. Vacuum bagging offers many advantages over conventional clamping or stapling techniques, such as uniform distribution of pressure, efficient lamination and the most important effect, to control the excess adhesive in laminate, resulting in higher fiber-to-resin ratios.

Figure 5.9: Vacuum bagging process.

Finishing this process, that has taken 8 hours as suggested from the technical data sheet to cure the resin at environmental temperature (25°), it is placed in a ventilated oven, to finish the curing procedure for 24 hours at 60°.

Once finished the curing time the specimen is ready to be removed from the allumium lamina and cut in specimen shape needed for the tensile test, as reported in ISO 527-4. Four specimens are obtained.

From Fig. 5.8 to Fig. 5.10 the different phases of composite preparation are shown.

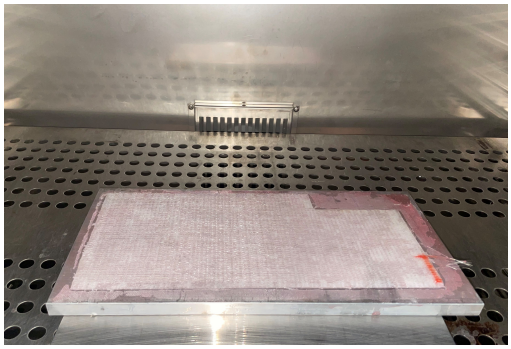

Figure 5.10: Curing process in oven.

Test of the specimen

To extract correctly all the mechanical properties of the specimen, DIC procedure or extensometers should be used, but for this specific case aiming to verify the consistence with TexGen simulation, it is considered enough to extract only longitudinal elastic modulus by a simple tensile test. Unfortunately the reduced dimensions of the material available does not allow a test in transversal direction too.

The specimen shape is rectangular, 25 cm in length and 2.5 cm for the width as suggested by ASTM 3039. The speed is set at 2 mm/min. The tests have been executed using a machine with hydraulic crimp system as shown in Fig. 5.11. From the tests, comparable results especially in elastic field are obtained, as it is the most relevant property aiming to characterize the composite elastic modulus.

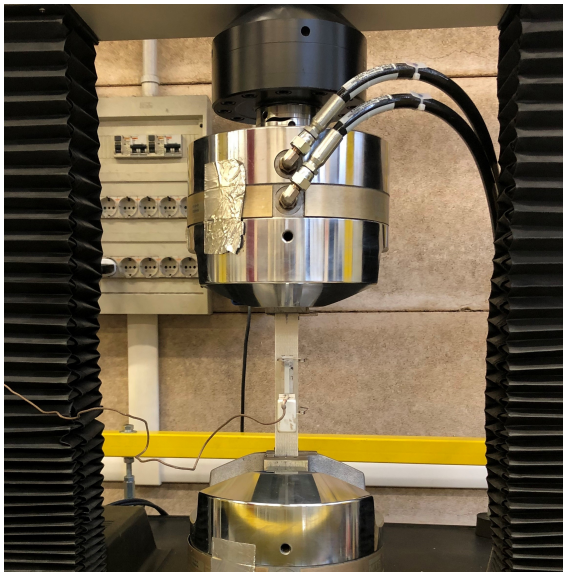

Figure 5.11: Tensile test.

In addition, a specimen (specimen B) is produced applying a certain pressure to simulate the real action of ski press, as it causes a variation in thickness and an increasing of the fiber volume fraction. In Fig. 5.12, stress strain diagram of these two different types of specimen are reported. As it can be seen, specimen B shows

an higher elastic modulus, that is coherent with theory of composites (Chapter 2).

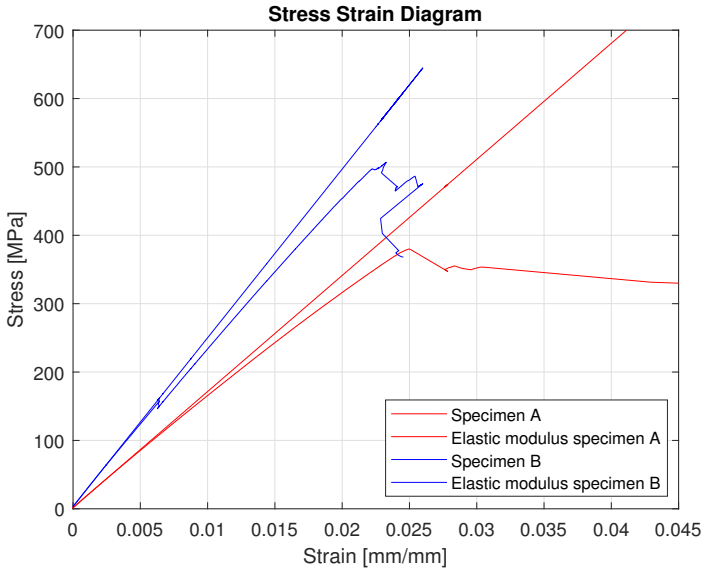

Figure 5.12: Stress strain diagram of glass fiber reinforced composites

Table 5.10: Experimental glass fiber composite Young's Modulus

Specimen	Elastic Modulus [MPa]
A	17000
B	24670

Tab. 5.10 addresses in a more explicit way the value of Young's modulus.

TexGen Simulation

As the experimental data are now available, it is possible to validate the results achieved with the simulation in Texgen. Unfortunately it is not possible to know the correctness of the properties in all directions, but it is useful to check at least the coherence of elastic modulus in longitudinal direction that is the most relevant information focusing on ski bending behaviour.

As already presented in Section 5.2.1, unit cell is created knowing all the dimensions from specimen given by the company (Fig. 5.13).

Table 5.11: Fiberglass unit cell geometry

Length $[mm]$	Width $[mm]$	Thickness $[mm]$	Volume $[mm^3]$
5.4	4.3	0.5	11.61

In Tab. 5.11, unit cell global dimension are provided, while Tab. 5.12 refers to the detailed dimension of each fiber. Differently from the basalt-glass composite unit cell, in this case the width and the section of fibers is different in vertical

and horizontal direction. This has the aim to increase its behaviour especially in longitudinal direction.

Table 5.12: Input data for yarn modeling - Fiberglass

Yarn Spacing $[mm]$	Yarn width $[mm]$	Fabric thickness $[mm]$	N° of Warp Yarns	N° of Weft Yarns
2.425	1.8	0.4	02	02

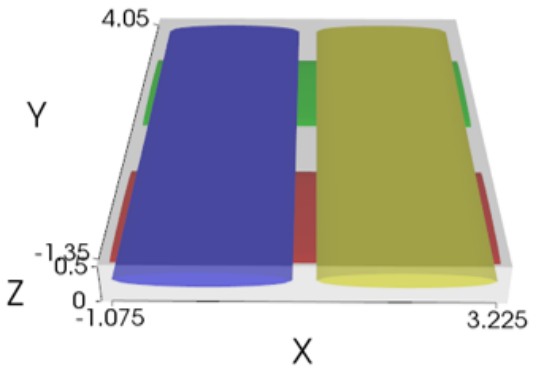

Figure 5.13: Unit Cell of the fiber glass composite.

The data obtained from the simulation are resumed in Tab. 5.13.

Table 5.13: TexGen glass fiber composite mechanical properties

Material	E_x [GPa]	E_y [GPa]	E_z [GPa]	G_{xy} [GPa]	G_{yz} [GPa]	G_{zx} [GPa]	ν_{xy} [-]	ν_{xz} [-]	ν_{yz} [-]
Glass fiber composite	18.3	26	6.37	6.44	1.95	1.93	0.12	0.3	0.29

It is now possible to make a comparison between the longitudinal modulus found experimentally and the one from numerical simulation. The error results around 5%. It is now reasonable to assume a correct approximation of the reality given by TexGen.

5.2.3 Steel edges

Steel edges are present in all skies, as they are fundamental in order to direction the turn and to have grip enough on ice snow conditions. The typical shape is represented in Fig. 5.14 and what immediately strikes the attention is its curvilinear aspect. The main reason should be addressed to the better grip with resin and materials layers.

Figure 5.14: Steel edges.

This shape becomes complex in FEM models due to a great amount of small radius, that means a lot of partitions in order to have simpler regions to be meshed. In addition, contact between steel edges and other materials appears to be difficult. Therefore a model with simplified geometry has been defined without compromising its stiffening effect.

This is possible through a simulation, considering the real shape and comparing its result with a simplification, obtained through an iterative procedure. Firstly the original shape has been created in Inventor, reproducing the effective geometry from the sample given by the company. Then the part is imported in Abaqus to be analysed. A properly partitioned edge depicted in Fig. 5.15 is tested.

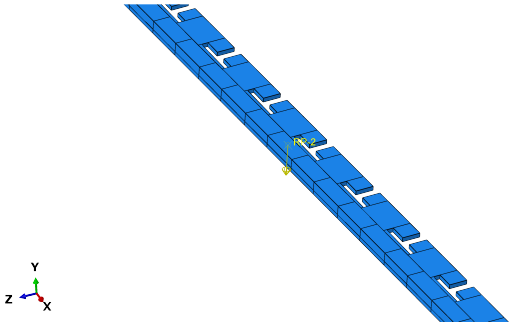

Figure 5.15: Steel edges in FEM.

Compared to the real one, round fillet are simplified as straight to allow a better mesh. The load condition is a three point bending test, that allows to consider only the stiffening role of the steel edges, without analysing its contribute in torsion. The applied load is 2.5 N, it is considered enough to have a reasonable deflection while remaining in the elastic field. As boundary condition, the final extremes were locked preventing every motion except for rotation around z axis. The result of deflection is represented in Fig. 5.16.

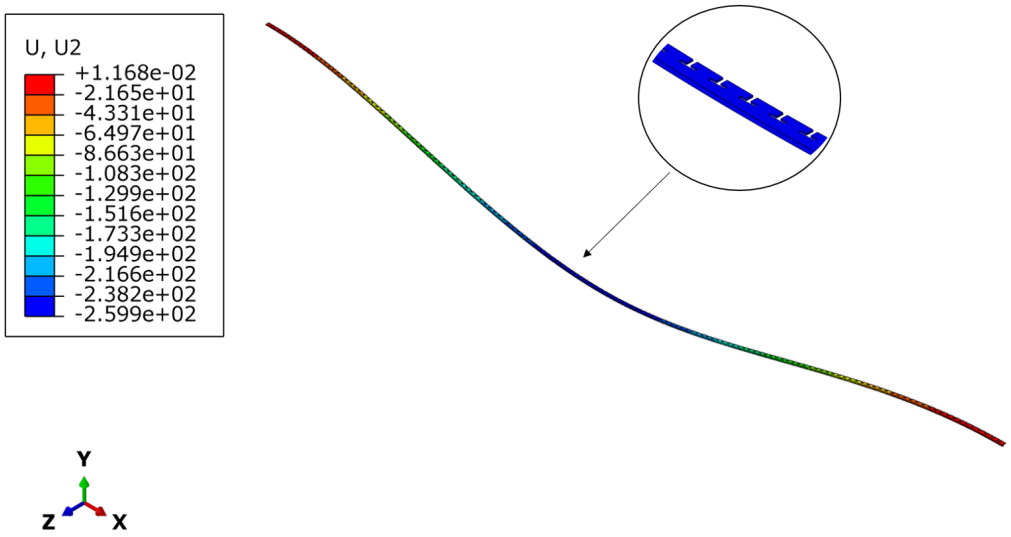

Figure 5.16: Deflection of the lamina.

Equivalent Model

Based on the results of real model, the objective is to find a good simplification through an iteration process looking to the best approximation of real deflection. The simplification consists in removing all the fillets and curved details, then the geometry can be reduced keeping the same elastic modulus or, as alternative, can be maintained equal changing the elastic modulus. In this case the first choice is selected.

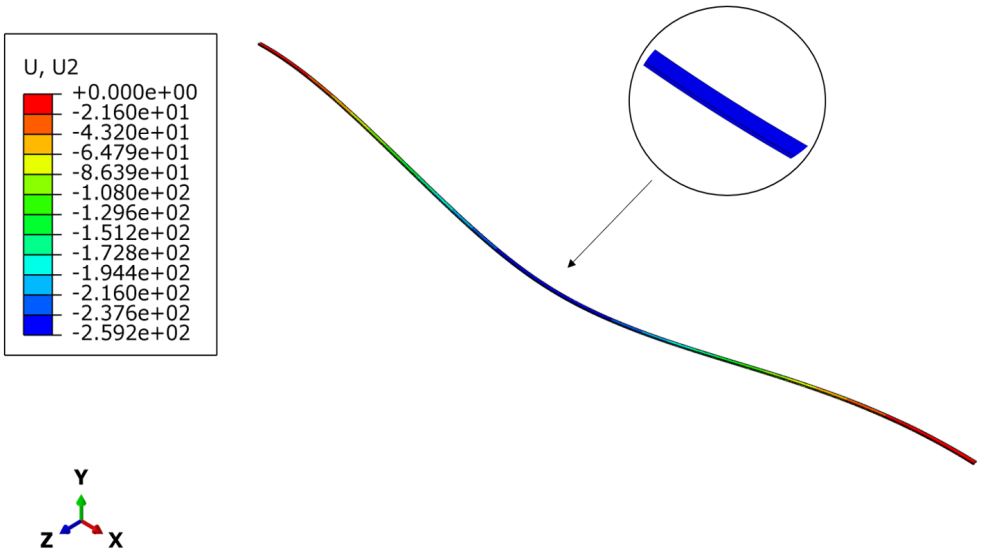

Figure 5.17: Deflection of the lamina simplified.

From the simplified model in Fig. 5.17, deflection shows a difference lower than 1% respect to the real model. Therefore, this new shape can be used for the ski model.

5.2.4 Remaining materials

For the remaining materials, the characterization follows the analysis made by Concli and Fraccaroli [18]. In their study, a strong but reasonable assumption was imposed by the lack of possibility to test specimen in thickness due to the low dimension. On this reasoning, materials were considered as transverse isotropic.

Considering xy as the longitudinal plane, transverse isotropy imposes:

$$E_y = E_z \tag{5.3a}$$
$$G_{xz} = G_{yz} \tag{5.3b}$$
$$\nu_{xz} = \nu_{yz} \tag{5.3c}$$

This assumption is typically used for wood, unidirectional composite, foams and minerals. As consequence, it can be applied correctly to Material 9, 24, 290, 139, 146, 207 (Fig. 5.2) that were effectively tested in longitudinal and transverse direction or as in case of steel edges whose mechanical behaviour is isotropic.

Tab. 5.14 resumes all:

Table 5.14: Ski materials mechanical properties

Properties	**9** **Nylon**	**24** **Glass Fiber composite**	**290** **Glass Fiber composite**	**139** **ABS**	**146** **Steel**	**207** **PE**
E_x [MPa]	550	35000	20000	800	206000	850
E_y [MPa]	567	8700	13700	750	206000	897
G_{xy} [MPa]	193.85	5160.29	7104.704	273.78	79230.7	6113.19
ν_{xy} [MPa]	0.45	0.23	0.18	0.45	0.3	0.42

5.3 Conclusions

This chapter enters in the characterization of SkiTrab Freedom 90 constituent material. Soft wood, composite and steel edges are treated proposing simulation and simplification of real parts creating a strong know-how. In particular, TexGen software is used to predict textile reinforced composite mechanical properties supported by an experimental test, while steel edges are tested and simplified in Abaqus.

Chapter 6

Experimental tests

After introducing the nature of the tested ski, an experimental procedure has been developed in order to have results to be compared with simulation results. As shown in Chapter 3 the main forces exerted on ski are bending and torsion, usually at the same time. Therefore, a bending test and a bending-torsion test are set. Test has been performed by simply considering the ski as a beam on two supports as schematic represented in Fig. 6.1.

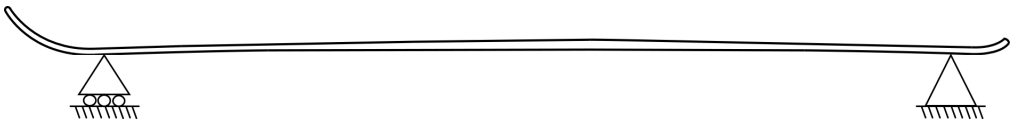

Figure 6.1: Ski configuration.

In the next chapter, to satisfy a high level of coherence with simulation, dimension of ski between supports is considered, neglecting both tip and tail. For both the tests a proper configuration is set concerning steel plate and supports.

6.1 Bending Test

Bending test is a method of testing materials for their bending strength and other important properties such as ductility or resistance to fracture. Bending tests are similar in their sequence, but depending on the number of pressure points and specimen support, a distinction is made:

- *one point bending test*
  Specimen is clamped at one end, while opposite extreme is loaded with the test punch. Flexural modulus or bending-elastic modulus is equal to the ratio of the maximum fiber stress to the maximum strain within the yield point.

- *three point bending test*
  This name is related to the three pressure points in setup, two supports and a centrally loaded test punch. The specimen lies crosswise on supports and protrudes at the sides. It is the most frequently performed bending test. However, it has the disadvantage that, in addition to the compressive and

tensile forces exerted, transverse forces are effective in the material. For this reason, four point bending test is developed.

- *four point bending test*
  Instead of the single punch applying force in the center as for three point bending test, a double punch is used. In the area between the two upper pressure points, a constant bending moment is formed avoiding presence of transverse forces.

In this specific case, three point bending test is performed. Ski is positioned aligned with the axis of test machine, the load is set to 120 N according to Concli and Fraccaroli [18]. It is transmitted through traverse machine movement at a speed of 10 mm/min. A load cell measures applied force. The right extreme of ski leaves only rotation around transversal axis as D.o.F, while left one allows both rotation around transversal axis and translation along longitudinal direction. This type of boundary is selected to avoid arc effect, caused by the impossibility of translational motion, that otherwise would stiff the structure, changing its real behaviour.

(a) *Front view* **(b)** *Lateral view*

Figure 6.2: Ski bending test

Fig. 6.2 shows how the bending test is performed, leaving the tip free to move, while fixing the longitudinal degree of freedom of the tail.

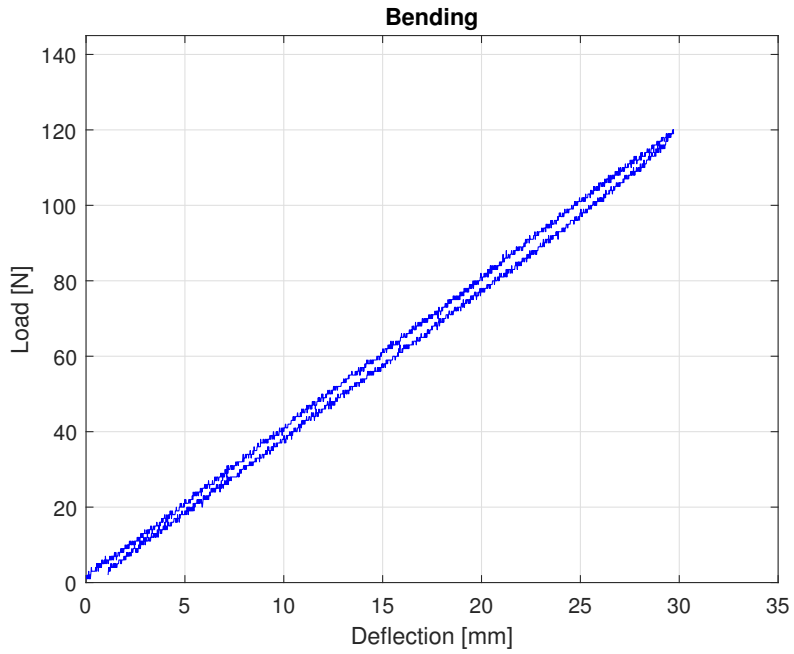

Figure 6.3: Ski deflection in bending condition with disturbances.

Some disturbances affect the Fig. 6.3 data introducing important errors in case of small load application. For this reason it is necessary to post process them as depicted in Fig. 6.4.

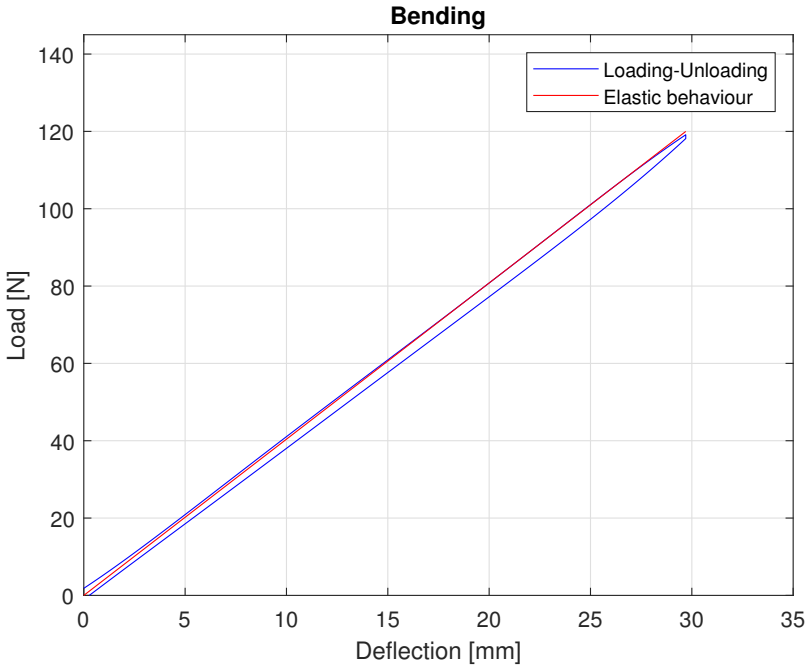

Figure 6.4: Ski deflection in bending condition.

6.2 Bending-torsion test

Usually the torsional resistance is tested through fixing the ski at boot center mark while an increasing torque is applied at the shovel until a torsion angle of about 8° is reached, which is a realistic torsional ski deformation during skiing. Torsion angle and torque is continuously recorded by a rotary potentiometer and a miniature ring load cell. As consequence, the torsional spring constant of the ski is derived from the maximum torsion angle and the applied moment. Alternatively, the moment can be applied to tip, fixing tail or viceversa.

The choice of bending-torsion test instead of pure torsion was done to overcome the lack of machines to test the ski in a condition of pure torsion. In order to transmit a twist, an out of plane load must be applied. In this case, the ski is set at a distance of 200 mm and using two bars to constrain the ski and to transmit the force, a torsion is generated. The force is set to 90 N. As effect both the contributes, deflection and rotation are obtained.

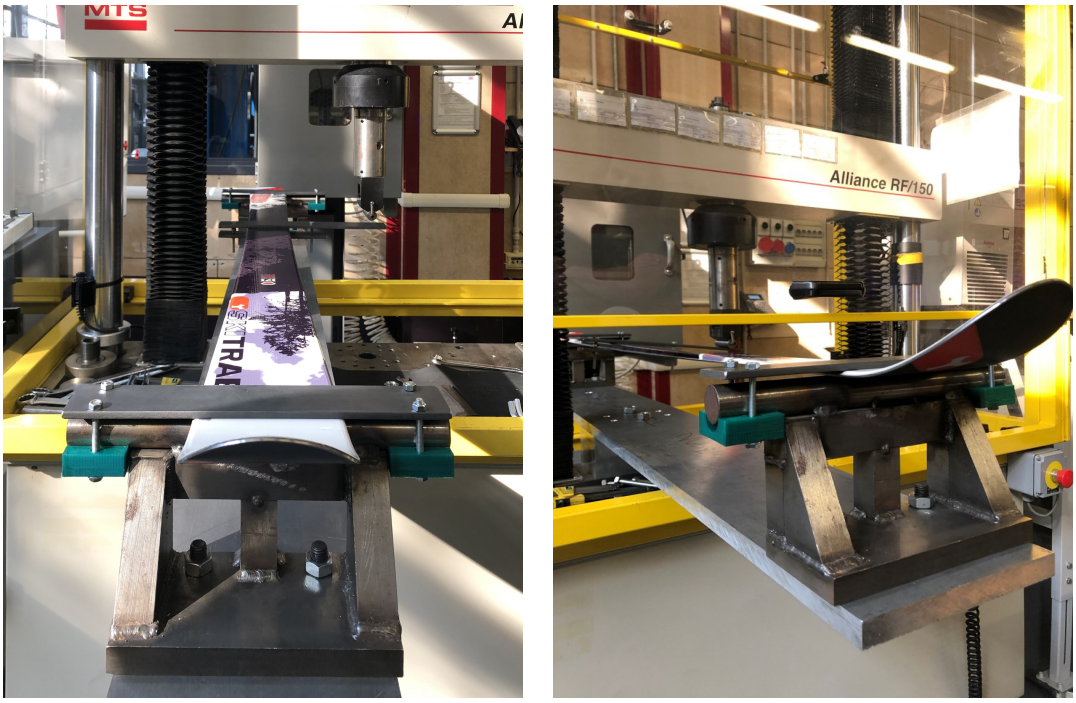

(a) *Front view* **(b)** *Lateral view*

Figure 6.5: Ski bending-torsion test.

As it can be seen in Fig. 6.5, boundary conditions are applied differently due to the need to lock ski preventing rotation around longitudinal axis. For this reason the clamping systems are applied both at tip and tail, leaving the possibility of translation along longitudinal axis anyway.

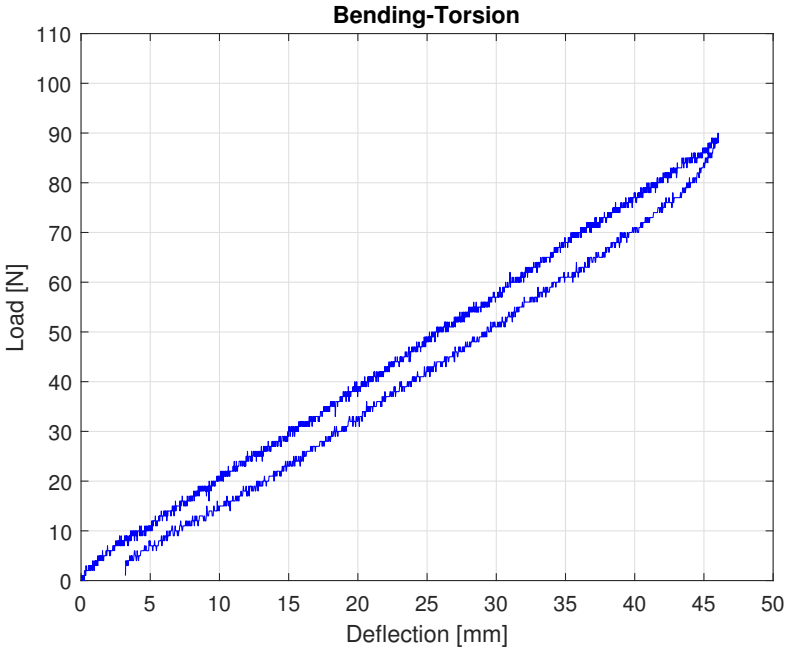

Figure 6.6: Ski deflection in bending-torsion condition with disturbances.

As already said, with low load intensity the disturbances become relevant as shown in Fig. 6.6. Therefore, as done before, a post operation to filter the signal is needed (Fig. 6.7).

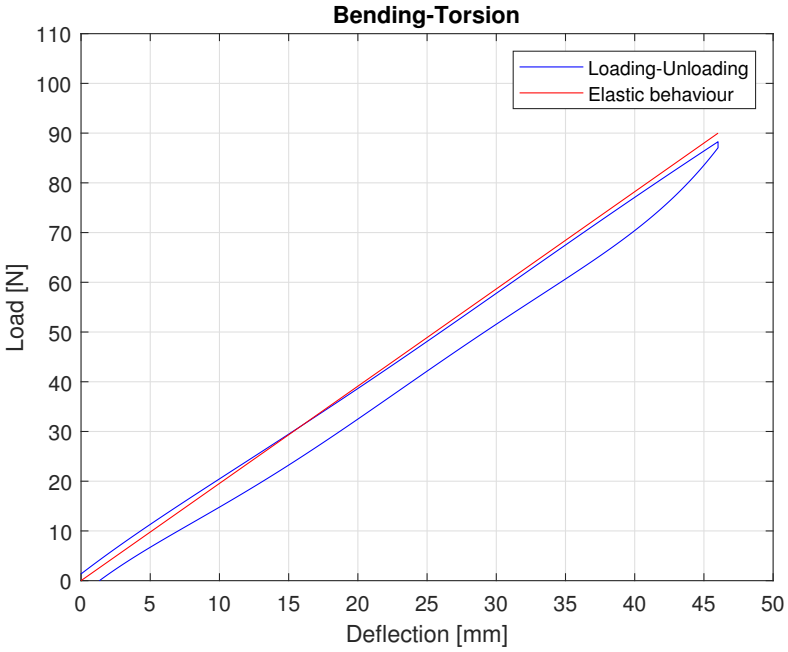

Figure 6.7: Ski deflection in bending-torsion condition.

For a more detailed configuration of the constraints for bending and bending-torsion tests see Appendix A.

6.3 Conclusions

This chapter presented the experimental campaign performed on the physical ski. Tab. 6.1 summarizes the results.

Table 6.1: Ski deflection

Test	Force [N]	Deflection [cm]
Bending	120	2.97
Bending-torsion	90 @ 200 mm	4.60

In Fig. 6.4 and 6.7 are underlined real and ideal behaviour that differs especially for the unloading phase. In fact, a sort of hysteresis is present. This happens in case of plastic deformation in which a residual strain is present due to the achievement of elastic limit during loading phase that implies a residual deformation once unloaded.

In this specific case it can be explained by considering that ski is not fixed, so having a certain freedom in translation the load application point could be different for the loading and unloading phase resulting in a residual deformation.

Chapter 7

Simulated ski models

[1] Being all the informations about ski geometry and section are available, a numerical model can be proposed. Starting from the knowledge of the production process, consisting in deposition of different materials layers joint together with proper epoxy resin, and knowing their thickness, a coherent model has been developed.

The geometry is computed in Inventor to reduce the time needed to create the model. A .sat file containing all the informations about the geometry is then imported in Abaqus. The division of layers is based on the creation of an offset starting from top and bottom. In this way the only part that remains is the core, which presents a variable profile.

The analysis consists in an initial validation of the elements for simulation, then ski is considered with progressive degrees of complexity. The reason behind the choice of not starting from the "official" model lies behind the necessity of understanding which kind of simplification gives reasonable results and reduces computational time and effort.

7.1 Comparison between shell and solid models

A first simple model, simulating bending and bending-torsion has been developed in order to compare the numerical solutions and check the coherence of solid and shell model. A single lamina will be considered addressing the properties of layer 24 (Tab. 5.14).

Tab. 7.1 lists the model geometry.

Table 7.1: Unidirectional Fiberglass Composite lamina geometry

Material	Length [mm]	Width [mm]	Thickness [mm]
24	1442	110	5

Both conventional and continuum shell models have been studied to be confident about the goodness of the element types.

[1] The main literature reference for this chapter is: *Abaqus Documentation* [15]

7.1.1 Bending

Boundary Conditions

Particular attention is given to the description of boundary conditions being the same used for final ski model simulation. As shown in Fig. 7.1, left and right extremes are different in terms of degrees of freedom, in fact the right one is free to move only in terms of rotation around z-axis, fixing all the remaining D.o.F, while left one enables the translation in x direction (roller-pin configuration). This choice that aims to recreate a coherent parallelism with the tests, wants to avoid the arc effect stiffening the structure.

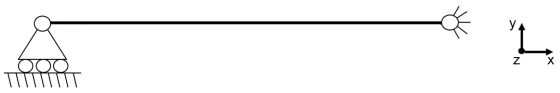

Figure 7.1: Scheme of bending constraint.

Boundary conditions consist in selecting the lateral edge and fix it, by removing the possibility of freedom in all the directions with exception of those ones previously mentioned. The selected lateral edge is the low one.

Load

Test consists in applying a load at the midspan of the lamina. Due to the combination of material properties and reduced thickness dimension compared to the characteristic length, a small load equal to 10 N is set. This is possible by connecting the selected point to a little portion of the part. The connection is realized using *Coupling Constraint*.

Within the surface-based coupling constraint, Abaqus provides coupling between a reference node and a group of nodes referred to as the "coupling nodes." The coupling nodes are selected automatically by specifying a surface and an optional influence region. The coupling constraint is useful when a group of coupling nodes is constrained to the rigid body motion of a single node. It is usually used to apply loads or boundary conditions and to model end conditions and interactions with other constraints. In Fig. 7.2, the choice of control point, surface and D.o.F. to constrain in coupling are shown.

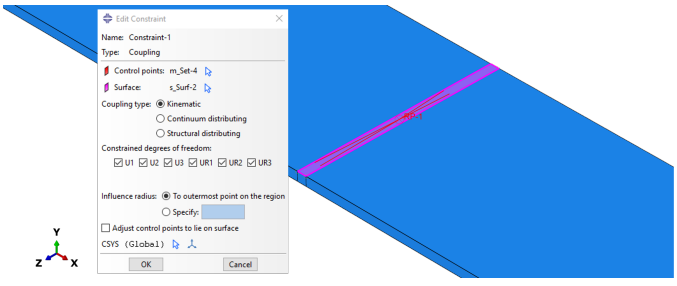

Figure 7.2: Coupling Constraint.

A kinematic coupling is applied. According to Abaqus Documentation [15], it constrains the motion of the coupling nodes to the rigid body motion of the reference

node. Kinematic constraints are imposed by eliminating degrees of freedom at the coupling nodes. Once any combination of displacement degrees of freedom at a coupling node is constrained, additional displacement constraints cannot be applied to any coupling node involved.

Results

Results are displayed in Tab. 7.2.

Table 7.2: Lamina bending deflection

Model	Element Type	Deflection [mm]
Solid	C3D8I	15.47
Conventional Shell	S4R	15.38
Continuum Shell	SC8R	15.47

The error among these three cases is lower than 1%.

On this basic model some considerations about elements used are proposed because they have been maintained for the final ski model. Starting from conventional shell elements, the lamina is discretized using *Linear reduced quadrilateral* element, corresponding to S4R in Abaqus, that can be considered a development of bilinear quadrilateral. It can model bending without causing over stiffness in the model. Quadratic option that corresponds to an increasing of node number from four to eight is not used because it is not necessary to complicate the element without reasoning and in addition both the solutions give the same deflection.

Continuum shell elements use *Linear reduced hexaedron* element, that is the equivalent of SC8R. The name hexaedron is not proper of 2D element, but it is related to its visualization mode. In detail it is an 8-node quadrilateral in plane. No quadratic option is present due to the inability to represent rotational degree of freedom.

Solid uses *Linear reduced* element, that is nothing more than trilinear hexaedron. As linear element the selected option is incompatible one, C3D8I in Abaqus, found to be more precise compared to reduced linear and fully linear.

In particular, incompatible mode elements represent a possibility to overcome the problems of shear locking in fully integrated, first-order elements. Since shear locking is caused by the inability of the element displacement field to model the kinematics associated with bending, additional degrees of freedom, enhancing the element deformation gradient, are introduced into linear class element. Therefore, a first-order element is allowed to have a linear variation of deformation gradient across the element domain. Indeed, the standard element formulation results in a constant deformation gradient across the element with the effect of nonzero shear stress associated with shear locking. This is possible without adding nodes, because the deformation gradients are internal to the element and not associated with nodes. Incompatible mode elements can produce results in bending problems that are comparable to quadratic hexaedron but at significantly lower computational cost. In particular, in this case quadratic elements produce the same displacement found with incompatible modes.

Alternatively, linear reduced integration can be chosen, corresponding to C3D8R, with an error of about 10% respect to C3D8I, in particular the lamina appears to be less stiff. It can be applied only to quadrilateral or hexahedral elements and consists in fewer integration point in each direction than the fully integrated elements. Locations of the integration points for reduced-integration, quadrilateral elements are shown in Fig. 7.3.

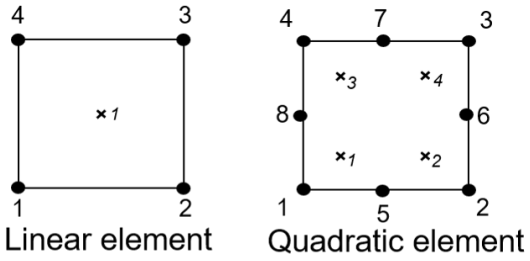

Figure 7.3: Reduced integration elements. [15]

Linear reduced-integration elements tend to be too flexible because they suffer a numerical problem called hourglassing (Fig. 7.4).

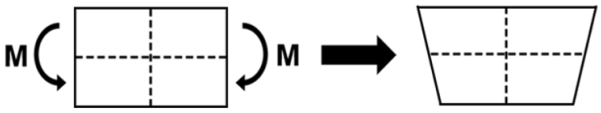

Figure 7.4: Hourglass. [15]

Either the dotted visualization lines has not changed in length, as well as the angle between them remains unchanged. Therefore, all stress components at the single integration point of the element are zero. Thus, bending deformation mode is a zero-energy mode because no strain energy is generated by this element distortion. The element is unable to resist this type of deformation since it has no stiffness in this mode. In coarse meshes, this zero-energy mode can propagate through the mesh, producing meaningless results. To overcome this issue, a small amount of artificial "hourglass stiffness" is introduced in first-order reduced-integration elements to limit the propagation of hourglass modes. This stiffness is more effective at limiting the hourglass modes when several elements are used in the model. Therefore, linear reduced-integration elements can give acceptable results as long as a reasonably fine mesh is used.

In this specific case, by enhancing the hourglass control, the result improves, converging to the solution found with C3D8I.

7.1.2 Bending-Torsion

Boundary Conditions

Boundary conditions are set equal to bending case.

Load

For bending-torsion simulation the lamina is subjected to bending and torsion. So, a combination of deflection and angular distortion will be present. This is realized in Abaqus by applying a force equal to 10 N on a point at a distance of 300 mm with respect to the longitudinal axis of the lamina and connected to a portion of lamina through kinematic coupling constraint. In this way the part undergoes to both the forces.

The decision to apply a force shifted from lamina center of mass, instead of a torque, is made in order to be coherent with the bending-torsion applied to the ski. In addition, continuum shells elements do not have the rotational degree of freedom, therefore a torque cannot be applied.

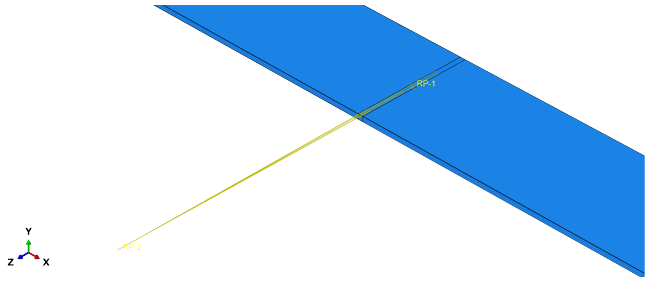

Figure 7.5: Coupling Constraint in bending torsion.

Results

Table 7.3: Lamina bending-torsion deflection

Model	Element Type	Deflection [mm]	Rotation [°]
Solid	C3D8I	28.67	2.509
Conventional Shell	S4R	28.72	2.527
Continuum Shell	SC8R	28.78	2.529

Once again results in Tab. 7.3 underline convergence among the three different model solutions. The element type choice is done following the same reasoning proposed for bending case.

7.2 Laminae model

This first model is the basic one and consists in the ski simply divided in different layers, each one corresponding to each material, recreating a sandwich structure (Fig. 1.3). However this configuration does not correspond to the reality because cages are effectively present in Freedom 90 model. The main advantage from a simulation point of view is a reduction of time process and a strong simplification for what concerns constraints that couple assembly different parts. The section of ski is reported considering this first approximation is reported in Fig. 7.6.

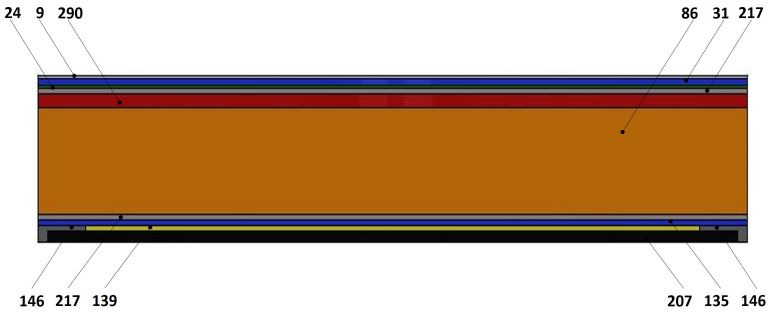

Figure 7.6: Ski section lamine.

Many of the existing ski models (Wolfsperger, Szabo, and Rhyner [24], Federolf [25]), focused on FEM ski response simulation, are based on this kind of structural model. Independently from the real ski architecture (Cap or Sandwich) this model is a good compromise in terms of computational time and accuracy. In order to simulate the resin that acts as a glue connecting all the layers, a rigid constraints between laminae has been selected, thus *Abaqus Tie Constraint* is implemented.

A surface-based tie constraint has been used to make the translational and rotational motion, as well as all other active degrees of freedom equal for a pair of adjacent surfaces. By default, nodes are tied only where the surfaces are close to one another. One surface in the constraint is designated to be the slave surface; while the other surface is the master surface. The default position tolerance for element-based master surfaces is 5% or 10% of the typical master facet diagonal length for the node-to-surface and surface-to-surface tie formulations, respectively.

In mechanical simulations, an unconstrained slave node can penetrate the master surface freely unless a contact is defined between the slave node and master surface.

The surface-to-surface approach generally involves more master nodes per constraint than the node-to-surface approach, which tends to increase the solver bandwidth in Abaqus and, subsequently, the computational effort. In most applications the extra cost is small, but the cost can become significant in case of large fraction of tied nodes (degrees of freedom) in the model, master surface being more refined than slave surface or multiple layers of tied shells, such that the master surface of one tie constraint acts as the slave surface of another tie constraint.

In a model with multiple tie constraint definitions, it is possible that the slave and master surfaces of different tie constraint definitions may intersect. If two tie constraint definitions have part or all of their master surfaces in common or if the surfaces tied are layered (i.e., the master surface of one tie constraint definition acts as the slave surface of a subsequent tie constraint definition), Abaqus attempts to chain the constraint definitions together. This will reduce the number of degrees of freedom and lower the computational expense, resulting, in faster run times. However, in a model with multiple tie constraint definitions, if nodes on the slave surface of one tie constraint definition are part of the slave surface of other tie constraint definitions, an overconstraint occurs. This error needs to be recognised and correct.

7.2.1 Laminae solid model

As already said, the model created in CAD environment has been imported in Abaqus via .sat file. After the assignment of materials and section, a proper partition has been developed in order to let the mesh to be the most accurate as possible. For bending, load condition and boundary conditions are applied as described in Section 7.1, while for bending-torsion load is applied in a slightly different way.

In order to simulate more correctly the real experiment an iron bar has been added (see Fig. 6.5). This has the function to transmit the moment to ski, making it twisting.

In the model, as it can be seen in Figure 7.7, the two bars are simplified as one. Obviously, this simplification is not coherent with the effective state of stress of the contact area bar-ski; but, being interested to the global behaviour of the ski, this absence of coherence results acceptable. In addition, only the protruding part plays a relevant role in the deflection of the two bars.

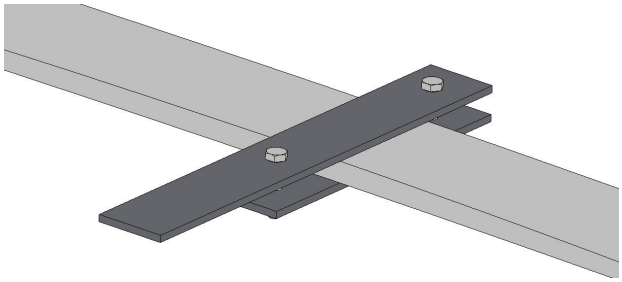

(a) *Bar ski real experiment*

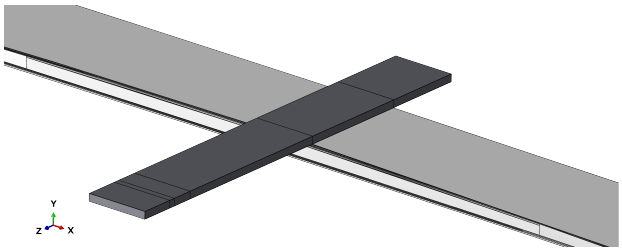

(b) *Bar ski Abaqus simulation*

Figure 7.7: Bar Ski interaction.

The bar is coupled with the ski through Tie Constraint, obviously the connection is adjusted due to the ski non planarity. The deflection highlighted is the one of the load application point, that is coherent with the experimental procedure.

In Fig. 7.8, the deflection of ski modelled with solid elements in bending condition is reported, while in Fig. 7.9, the global displacement of bar-ski system is depicted, while the load application point displacement is indicated in Tab. 7.5. This distinction is fundamental to provide a correct parallelism with the experimental procedure.

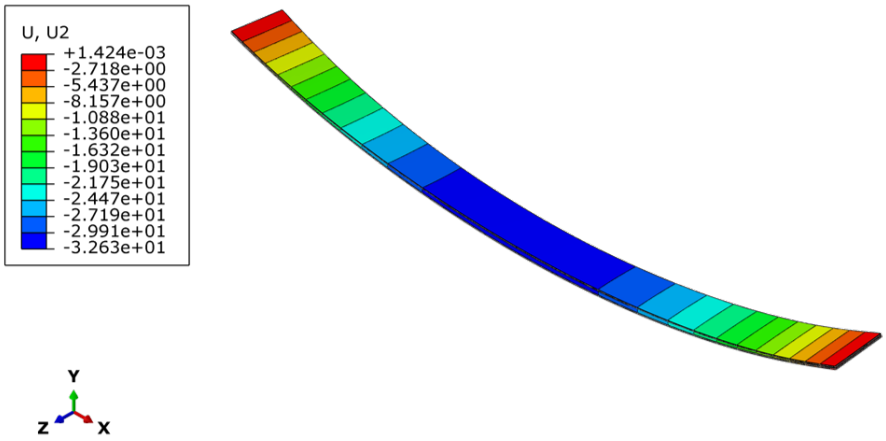

Figure 7.8: Bending solid laminae model.

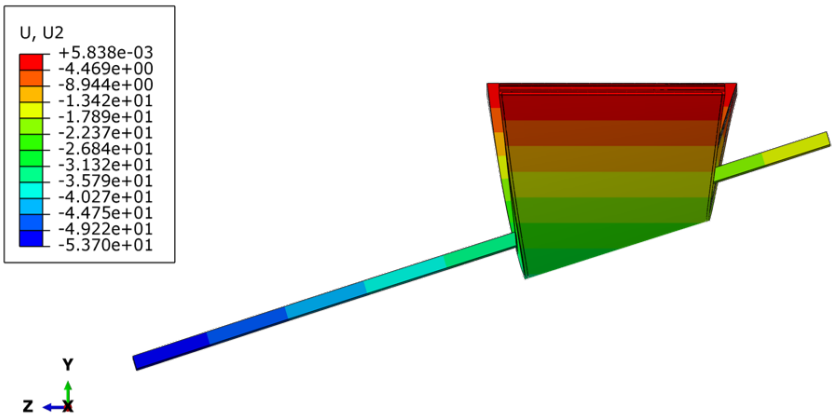

Figure 7.9: Bending-Torsion solid laminae model.

7.2.2 Laminae shell model

The model developed using conventional shell is the easiest in terms of each single layer shape. They appear like flat rectangular connected each other. Laminae are bounded by Tie Constraints, which needs to define a master and slave surface. For 2D element case, it means that upper and lower faces are treated as different surfaces in order to be considered as master and slave, thus realizing the desired constraint.

Two are the problems related to this type of element:

1. *different model respect to the solid one.*

   In fact, being 2D laminae, the operation, starting from 3D element, consists in removing upper and lateral faces leaving only the lower one. This causes a considerable waste of time, considering also that connections cannot be the same used in solid modelling, but they must be converted to the new parts shape.

2. *variable thickness definition.*

   Abaqus allows to build the part profile by creating an Analytical field consisting of an equation or of a set of points recreating the actual lamina profile. In ski specific case, the only variable lamina is wood, while all the other are characterized by constant thickness. This variable thickness leads to an increasing of computational time and as well as time to practically create the model.

Therefore, especially for the second problem that increases greatly the simulation time, the element choice is shifted to continuum shell elements that allows to treat the ski as 3D, while assigning the properties of a 2D lamina. The great advantage is the possibility to use the already done 3D model, changing only the definition of material and section, that must be proper of a shell part.

Fig. 7.10 and Fig. 7.11 show the displacement after load application and results resumed in Tab. 7.5.

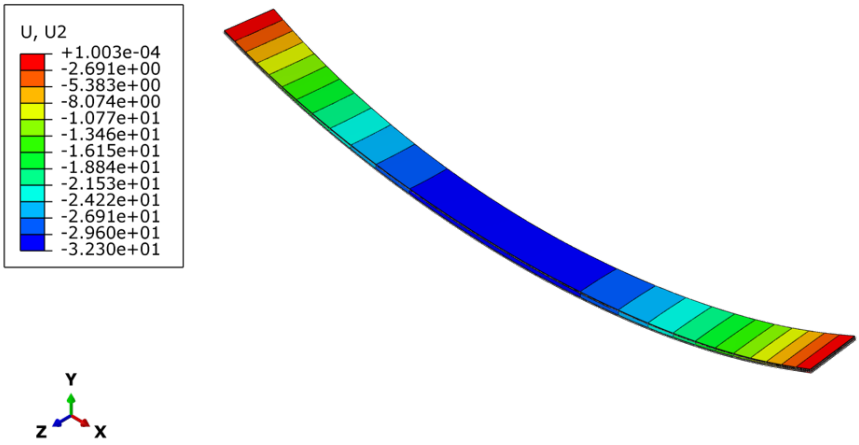

Figure 7.10: Bending shell laminae model.

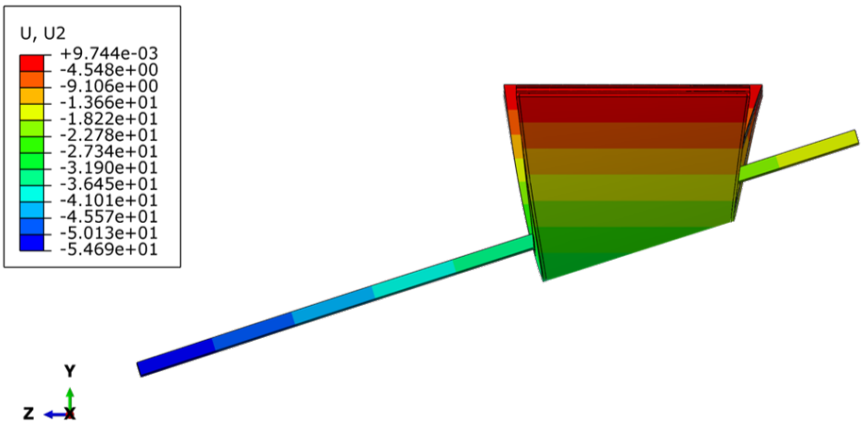

Figure 7.11: Bending-Torsion shell laminae model.

7.3 Cage model

With name "cage", the reference is to ski section, in which some elements present this kind of shape characterized by both horizontal and vertical part. In particular part 9, 31 and 217 made of plastic, glass fiber reinforced composite and glass-basalt fiber reinforced composite respectively are characterized by this added complexity (Fig. 7.12).

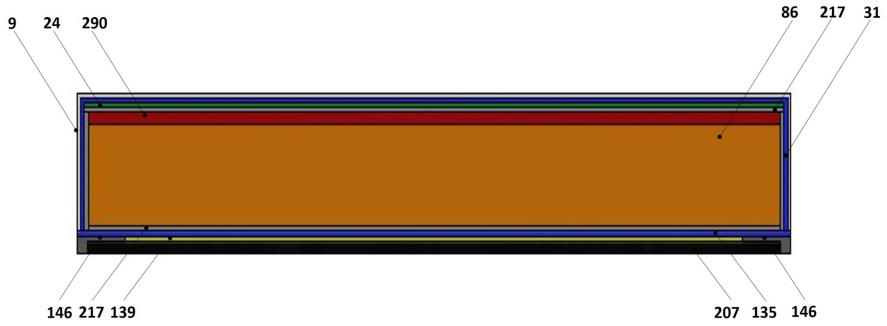

Figure 7.12: Ski section cage.

Beside a technical need to perform such a shape to better enclose all materials (Cap construction), the other reasoning is more oriented to gain additional stiffness in torsion, as declared by the company itself. To analyse if the role of cages in the model is effectively important, a simpler simulation has been proposed in the following section.

7.3.1 Reasoning on cage contribute

Before studying the ski with its new shape, it is reasonable to focus on the real advantages of cage. The attention of this little model is focused on torsion, because vertical parts, due to their low dimension, give a lower contribute to the bending stiffness respect to the parts placed horizontally. In this example a moment is applied to a steel structure having two different shapes, the first one is simply a lamina and the second one is characterized by this new shape as represented in Fig. 7.13.

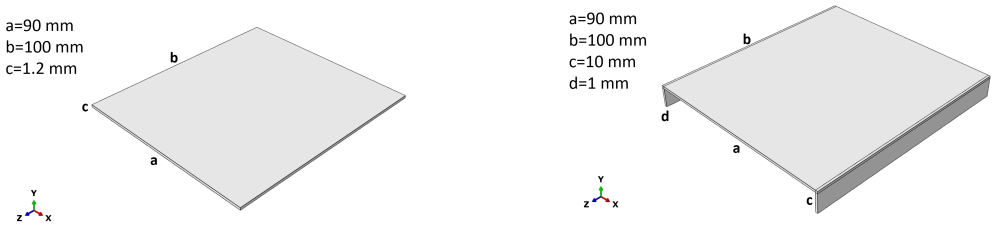

(a) *Lamina* **(b)** *Cage shape*

Figure 7.13: Comparison of different profile shapes.

It is important to underline that both structures have the same volume in order to set the same conditions in terms of mass. The results, listed in Tab. 7.4, respect

the expectations, as the rotation obtained by cage model is 30% lower than rotation of the other model.

Table 7.4: Angular deflection

Shape	Element Type	Rotation
Lamina	C3D8I	7.84°
Cage	C3D8I	2.47°

At this point, the second preliminary model is based on recreating the cage structure effectively present in ski, in which wood is enclosed (Fig. 7.14). Once again volume of the whole assemble is the same.

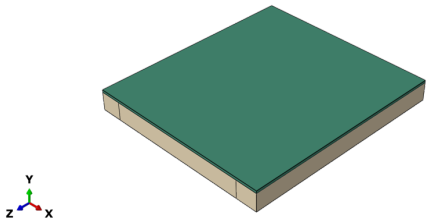

(a) *Lamina and wood combination*

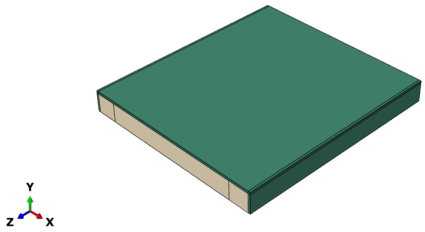

(b) *Cage and wood combination*

Figure 7.14: Comparison of different combinations.

Results after torque application highlights a rotation reduction of about 35% thanks to cage presence.

This explains, in a numerical way, the effect of cage addition, enclosing all the layers and giving additional torsional resistance to the whole model. Obviously the effective behaviour depends on the type of material, length and how the parts are assembled together. For instance, if aluminium is used the impact of cage is around 15% while if the assembly dimensions increases significantly in terms of length, the steel cage produces a rotation reduction of 10%.

To really understand the effective advantage of the cage, it is necessary to analyse the specific ski case.

7.3.2 Cage solid model

FEM simulation of the cage model are computed using the same boundary conditions and load used in Section 7.2.1. Their results are shown in Fig. 7.15 and Fig. 7.16.

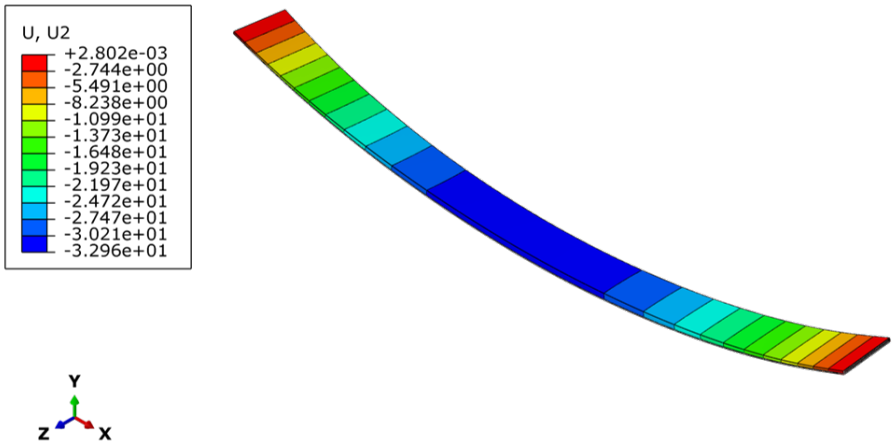

Figure 7.15: Bending solid cage model.

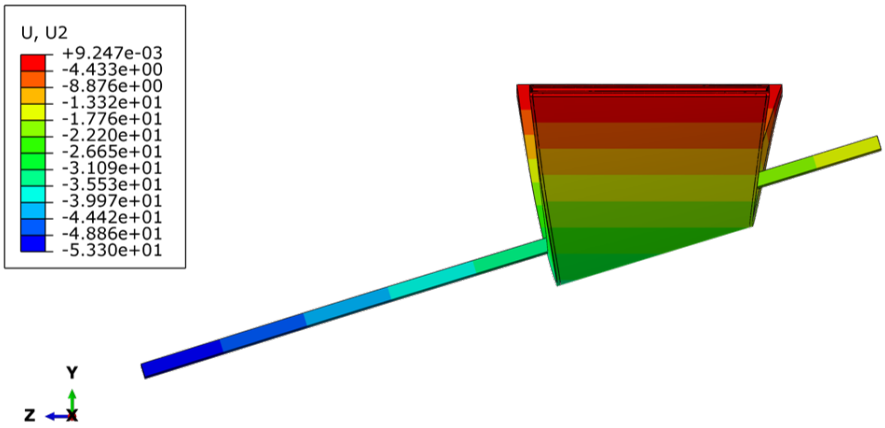

Figure 7.16: Bending-Torsion solid cage model.

7.3.3 Cage shell model

Differently from the laminae shell model discussed above, in which there were two possibilities to represent the ski using both conventional and continuum elements, in this case, the solution adopted requires the choice of continuum shell elements, because connection between layers cannot be accomplished by the use of simple 2D elements, due to the large amount of approximation introduced. The great advantage is based on the selection of a different surface for master and slave, reducing redundancy and providing the possibility to realize lateral coupling that are not feasible with conventional model due to the bad quality connection of edges with surfaces. The deformation modes are highlighted in Fig. 7.15 and Fig. 7.18.

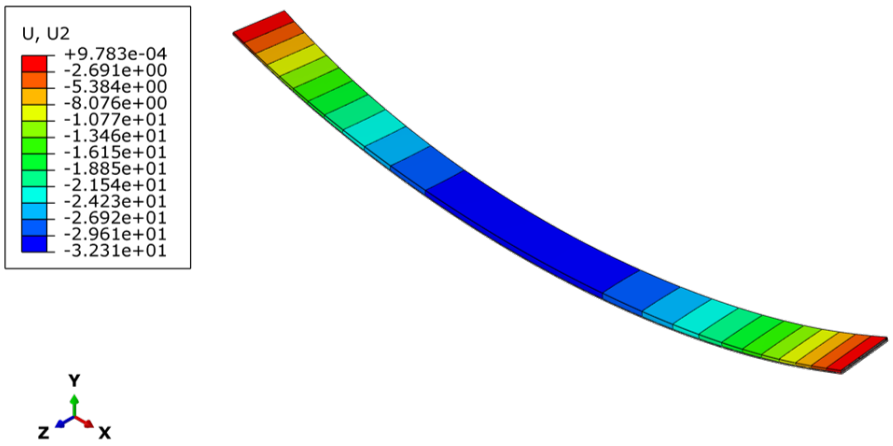

Figure 7.17: Bending shell cage model.

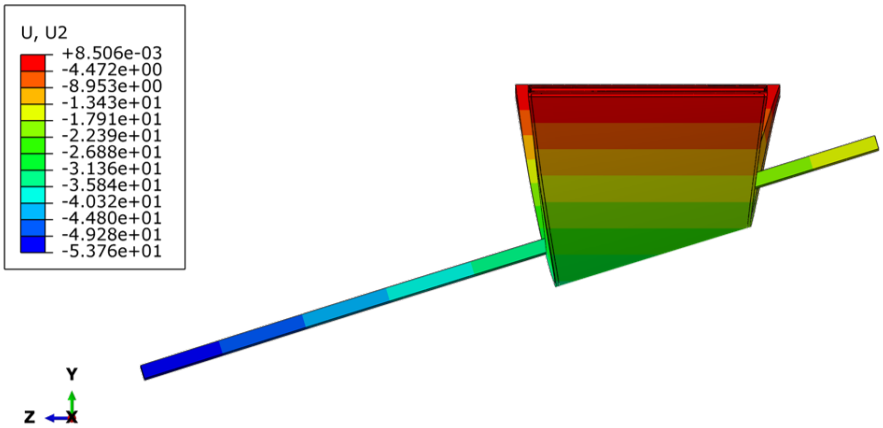

Figure 7.18: Bending-Torsion shell cage model.

7.3.4 Resume

Table 7.5: No camber ski displacements

Model	Solid laminae	Shell laminae	Solid cage	Shell cage
Element Type	C3D8R	SC8R	C3D8R	SC8R
Bending [mm]	32.63	32.30	32.96	32.31
Δ Error	9.9%	8.7%	11.0%	8.7%
Element Type	C3D8I	SC8R	C3D8I	SC8R
Bending-Torsion [mm]	49.76	50.62	49.42	49.84
Δ Error	8.2%	10.0%	7.4%	8.3%

The results of the deflections for every different model are reported in Tab. 7.5, as well as the amount of error respect to the experimental results.

It can be seen a coherence in terms of displacement between solid and shell model. This is related to the correct approximation of layers, being flat parts, with shell elements.

7.4 Camber ski

The simulations done in the previous sections do not consider the presence of camber effectively present, as reported in Chapter 5. Therefore, further simulations in which this aspect is considered have been performed, according to the same reasoning of the above section in terms of boundary conditions and loads.

The initial sketch is modified to consider this aspect. Even if, as discussed in Chapter 3, it is correct to assume that this detail plays an important role in case ski approaching a turn.

Table 7.6: Camber ski displacements

Model	Solid laminae	Shell laminae	Solid cage	Shell cage
Element Type	C3D8R	SC8R	C3D8R	SC8R
Bending [mm]	32.84	32.38	32.76	32.39
Δ Error	10.6%	9.0%	10.3%	9.1%
Element Type	C3D8I	SC8R	C3D8I	SC8R
Bending-Torsion [mm]	48.85	49.57	48.19	48.38
Δ Error	6.2%	7.8%	4.8%	5.2%

7.5 Conclusions

In this chapter a numerical model of the ski has been proposed, with a particular focus on the theory behind FEM. Element connections, constraints and elements choice have been discussed. The ski has been complicated step by step trying to recreate the real structure. Eight models have been studied, starting from a ski without camber and with a simplified materials arrangement, up to consider the real curvature and real layers geometry.

As it can be seen from Tab. 7.6, the developed models show that there is not difference in results respect to the models neglecting camber. It implies that the camber does not play any significant role in the flexural and torsional behaviour of the ski in static condition.

In addition the impact of cage has been observed to be quiet null, this can be addressed to its low dimensions and to the materials selected, which do not show high elastic properties compared to other materials that could have a bigger impact. This leads to conclude that, in this specific case, the real aim of cages is to protect core from environmental degradation.

Lastly, the maximum error with experimental data is about 11%, with better convergence for camber model especially in bending-torsion case.

Chapter 8

Conclusions

Ski production, also for high level ski, is mainly handmade, focused on the manufacturer experience and on experimental testing results. This thesis represents a preliminary study intended to demonstrate the possibility to realize numerical models to predict the ski behaviour, without the aim to diminish artisan experience, but to provide additional method to pre-screen possible solutions.

On these basis, following steps have been realized: as first analysing the ski production, then studying the applied loads during skiing, testing of materials employed, testing of the whole ski and finally defining different numerical models, aiming to recreate the real ski structure.

The real benefit of numerical model is the opportunity to work on each single component, that is not possible to monitor during ski testing, in which the whole system is observed.

However, nor the numerical models nor the real testing alone can offer a full understanding of ski potentiality. This represents the true core of this work, emphasizing the need to connect two worlds and creating a perfect mix of skilled craftsmanship and scientific research.

Further developments

For this purpose, all the following steps are linked to the increasing of model complexity, with the aim, in future, to monitor the athlete skiing action thanks to the measuring acquisition system mounted on the ski.

Before arriving to this final application, some easier improvements can be analysed. For example focusing on dynamic aspects, the use of natural fibers is proposed, in fact if the aim is to obtain a model suitable for racing both for the advantages in uphill and downhill phase, flax may be used. It offers great properties in terms of vibration damping and weight saving, with low cost and low environmental impact. Thanks to simulation this can be verified and checked.

In addition interaction with snow must be studied, observing ski behaviour in its working condition. This is fundamental because, depending on snow quality (hard, powder or spring snow), the interaction with ski will change, and some solutions will be preferred depending on the field of interest.

Through a mathematical model it is possible to work on each single component, that is not possible to monitor during ski testing in which the whole system is

observed. This is the true value of this work, to connect two worlds and create a perfect mix of skilled craftsmanship and scientific research.

Appendix A

Scheme of constraints

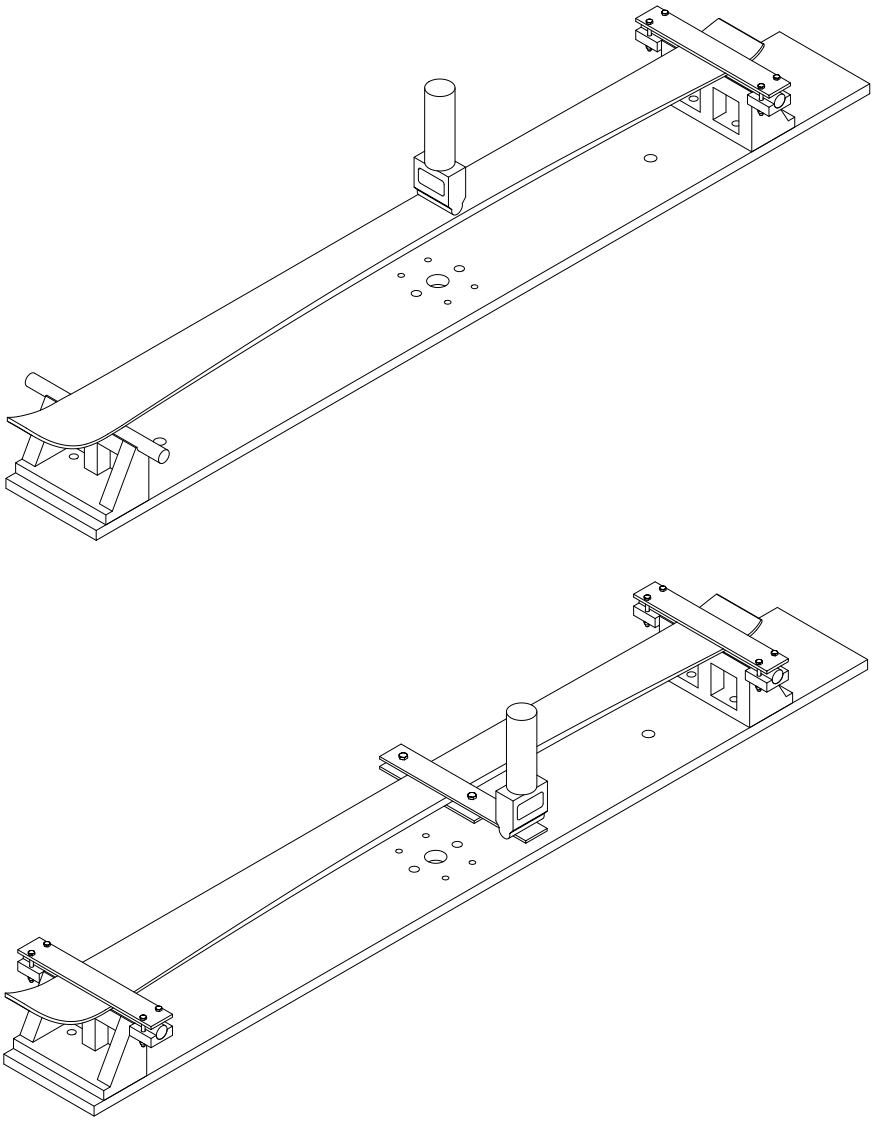

Acronyms

UHMWPE	Ultra High Molecular Weight PolyEthylene
UV	Ultraviolet Radiation
ABS	Acrylonitrile Butadiene Styrene
PU	Polyurethanic foams
NCF	Non-crimp fabric
UVO	Ultimate Vibration Object
ECM	Energy Management Circuit
FEM	Finite-element Method
Abaqus ©	Software suite for finite element analysis and computer-aided engineering
MWK	Multiaxial warp-knit fabric
D.o.F.	Degree of freedom
DIC	Digital Image Correlation
CSM	Chopped strand mat
CST	Constant Strain Triangle
LST	Linear Strain Triangle
Q4	Bilinear quadrilateral
Q6	Improved bilinear quadrilateral
Q8	Quadratic quadrilateral
TexGen	Open source software for modelling the geometry of textile structures

Bibliography

[1] C. Burkett. *Ski Construction: What Are Skis Made Of?* 2021. URL: https://snowlink.com/ski-construction/ (cit. on p. 3).

[2] *Gearwise: Skis*. 2015. URL: https://freeskier.com/stories/gearwise-skis (cit. on p. 8).

[3] *Mechanics of sport*. URL: http://www.mechanicsofsport.com (cit. on pp. 10, 12, 13).

[4] P. K. Mallick. *Fiber-reinforced composites: materials, manufacturing, and design*. CRC Press, Nov. 2007. ISBN: 9780849342059 (cit. on pp. 15, 19, 30).

[5] A. R. Horrocks. *Handbook of Technical Textiles*. Elsevier Science, 2016. ISBN: 9781782424659 (cit. on pp. 15, 21).

[6] *Reinforcement and Resin Systems*. 2013. URL: http://www.ericgreeneassociates.com/images/3._Reinforcements_and_Resin_Systems.pdf (cit. on p. 22).

[7] V. Nikitin. *Ski sidecut radius and radius of a carved turn*. URL: http://diginfo.ru/en/alpine-ski/ski-sidecut-radius-and-radius-of-a-carved-turn/# (cit. on pp. 25, 26).

[8] *Souplesse et Rigidité des skis: conséquences*. 2015. URL: https://marseille.glissattitude.com/blog/souplesse-rigidite-ski-consequences.html (cit. on p. 27).

[9] M. De Gobbi and N. Petrone. 'Acquisizione ed analisi del comportamento flessotorsionale di tavole da sci in slalom'. In: (2007) (cit. on p. 27).

[10] W. Nachbauer et al. 'Effects of ski stiffness on ski performance'. In: (2004) (cit. on p. 27).

[11] *Atomic Ski*. URL: www.atomic.com (cit. on p. 29).

[12] *Völkl Ski*. URL: https://www.voelkl.com/it/ (cit. on p. 29).

[13] *Head Ski*. URL: https://www.head.com/it_IT/ski.html (cit. on p. 29).

[14] R. D. Cook. *Finite element modeling for stress analysis*. Wiley, 1995. ISBN: 9780471107743 (cit. on pp. 31, 33–35, 37, 39).

[15] *Abaqus Documentation*. URL: https://abaqus-docs.mit.edu/2017/English/SIMACAEEXCRefMap/simaexc-c-docproc.htm (cit. on pp. 32, 39, 63, 64, 66).

[16] *Buyer's Guide 2014*. 2014. URL: https://issuu.com/mulateroeditore/docs/test2014 (cit. on p. 41).

[17] *Skitrab*. URL: http://www.skitrab.com (cit. on pp. 41–43).

[18] F. Concli and L. Fraccaroli. 'Introduction of Open-Source Engineering Tools for the Structural Modeling of a Multilayer Mountaineering Ski under Operation'. In: *Applied sciences* 10.15 (2020). DOI: 10.3390/app10155310 (cit. on pp. 42, 56, 58).

[19] W. Wu et al. 'Applying periodic boundary conditions in finite element analysis'. In: *SIMULIA community conference, Providence*. 2014, pp. 707–719 (cit. on p. 44).

[20] D. Mounier et al. 'Evaluation of transverse elastic properties of fibers used in composite materials by laser resonant ultrasound spectroscopy'. In: *Acoustics 2012*. 2012 (cit. on p. 44).

[21] P. Valentino et al. 'Mechanical characterization of basalt fibre reinforced plastic with different fabric reinforcements - Tensile tests and FE-calculations with representative volume elements (RVEs)'. In: vol. XXII. Gruppo Italiano Frattura, 2013, p. 231 (cit. on p. 44).

[22] P. Niemz et al. 'Physical and mechanical properties of common ash'. In: *Wood Research* (2013). URL: http://www.centrumdp.sk/wr/201404/13.pdf (cit. on p. 46).

[23] W. Green D, J. E. Winandy, and D. E. Kretschmann. 'Mechanical Properties of Wood'. In: Wood handbook—Wood as an engineering material. U.S. Department of Agriculture, Forest Service, Forest Products Laboratory, 1999 (cit. on p. 48).

[24] F. Wolfsperger, D. Szabo, and H. Rhyner. 'Development of Alpine Skis Using FE Simulations'. In: *Procedia engineering* 147 (2016), pp. 366–371. DOI: 10.1016/j.proeng.2016.06.314 (cit. on p. 68).

[25] P. A. Federolf. 'Finite element simulation of a carving snow ski'. PhD thesis. 2005 (cit. on p. 68).

[26] L. Shuguang and W. Anchana. 'Unit cells for micromechanical analyses of particle-reinforced composites'. In: *Mechanics of materials* 36.7 (2004), pp. 543–572. DOI: 10.1016/S0167-6636(03)00062-0.

[27] A. Dixit, H. S. Mali, and R. K. Misra. 'Unit Cell Model of Woven Fabric Textile Composite for Multiscale Analysis'. In: *Procedia engineering* 68 (2013), pp. 352–358. DOI: 10.1016/j.proeng.2013.12.191.

[28] D. Ferreira et al. 'Tensile strength of pine and ash woods – experimental and numerical study'. In: (2015).

[29] M. Barburski, M. Urbaniak, and S. K. Samal. 'Comparison of Mechanical Properties of Biaxial and Triaxial Fabric and Composites Reinforced by Them'. In: *Fibres and Textiles in Eastern Europe* 27.1(133) (2019), pp. 37–44. DOI: 10.5604/01.3001.0012.7506.

[30] T. Yokoyama and K. Nakai. 'Evaluation of in-plane orthotropic elastic constants of paper and paperboard'. In: *Dimensions* 60 (2007).

[31] S. Koman and S. Feher. 'Physical and mechanical properties of Paulownia clone in vitro 112'. In: *European Journal of Wood and Wood Products* 78.2 (2020), pp. 421–423. DOI: 10.1007/s00107-020-01497-x.

[32] M. Montagnin. 'Studio dei materiali impiegati nella costruzione di sci'. PhD thesis. 2011.

[33] P. Lorenz. *The truth behind carving!* 2013. URL: https://www.paullorenzclinics.com/post/the-truth-behind-carving.

[34] *The Truth Behind Carving!* 2019. URL: https://www.wheretogoskiing.com/the-truth-behind-carving/.

[35] *The Carving Skis*. URL: https://www.skileb.com/tips/carving-skis/.

[36] *Le resine epossidiche*. 2015. URL: https://www.nautechnews.it/2015/03/09/le-resine-epossidiche/.

[37] *Ski Camber Explained: Which Profiles are Best for Which Styles?* 2019. URL: https://skiprofiles.com/ski-camber-explained-whats-best-for-your-style/.

[38] *Ski shape and profile*. URL: https://www.gearx.com/blog/knowledge/skiing/ski-shape-profile/.

[39] *Ski camber vs. rocker: a skier's guide*. URL: https://www.wagnerskis.com.

[40] J. Ives. *Folsom's Guide to Ski Sidewall Construction*. 2020. URL: https://www.folsomskis.com/folsoms-guide-to-ski-sidewall-construction.

[41] *What gives a ski its character?* 2018. URL: https://www.genuineguidegear.com/life/blog/g3/what-gives-ski-its-character.

[42] *Ski flex: torsion vs. bending*. 2014. URL: http://blog.sandwichtechskis.com/2014/03/ski-flex-torsion-vs-bending.html.

[43] *Bending test: Suitable for both brittle and ductile materials*. URL: https://www.gom.com/en/topics/bend-test.

[44] *TexGen Documentation*. URL: http://texgen.sourceforge.net/index.php/Documentation.

[45] *Lay-Up Methods For Fibreglass (GRP) Composites*. URL: https://www.resinlibrary.com/articles/lay-up-methods-for-fibreglass-grp-composites/.

[46] William F Smith et al. *Scienza e tecnologia dei materiali*. McGraw-Hill, 2008.

[47] *Ski Construction: A Real Look at What's Inside Your Skis*. URL: https://theskimonster.com/blog/posts/ski-construction-a-look-inside-your-skis/.

[48] *ISO Standards*. URL: https://www.iso.org/standards.html.

[49] *ASTM Standards Publications*. URL: https://www.astm.org/Standard/standards-and-publications.html.

Ringraziamenti

Un grazie sincero ai miei genitori, per la pazienza con cui mi hanno accompagnata in questi anni, incoraggiandomi costantemente e supportandomi o per meglio dire sopportandomi, anche nei giorni più difficili.

A mio fratello, che oltre ad essere stato una reale fonte di ispirazione per la sua tenacia e dedizione, mi ha offerto sempre, talvolta nolente, un confronto importante per ogni esame.

Alle mie compagne di basket, che mi hanno accompagnato dal primo al quinto anno di Università, che mi hanno vista maturare, che hanno saputo essere il mio sostegno nei momenti di debolezza. Sono convinta che senza i nostri allenamenti, le trasferte, i postpartita, le risate (e qualche birra) mi sarei sentita meno leggera e pronta per affrontare questa sfida continua.

A Luca, mio costante compagno di studi degli ultimi due anni, con cui però ho condiviso molto di più che un semplice percorso didattico, ho condiviso vittorie, sconfitte, frustrazioni, risate, per non dimenticare una magica esperienza al parco avventura. Per queste e tante altre piccole cose, ne è nata un'amicizia che sono certa caratterizzerà per sempre la mia vita.

A Simone, la prima persona che ho conosciuto nel mio percorso al Politecnico e che purtroppo o per fortuna, mi ha cambiato la vita. Mi ha insegnato ad essere curiosa, a non sentirmi mai arrivata, a continuare a mettermi in discussione e non vedere mai nessun obiettivo come irraggiungibile. Grazie per questi anni indimenticabili.

A tutti i miei compagni del Poli, tra cui Riccardo, Davide e Alessandro compagni di caffè, aperitivi, viaggi in treno e tante risate, ossigeno puro dopo ore sui libri. Con loro ho avuto il piacere di condividere momenti che porterò sempre con me.

Grazie a chi mi ha visto iniziare questo percorso e che ora non c'è più, ma il cui ricordo mi è stato di stimolo per continuare e non arrendermi mai.